FRSH: A Frugal and Rapid bioSensor for in-House use to assess meat spoilage

Alaa Sarah Selim

A
Thesis in the Department
Of
Biology

Presented in Partial Fulfillment of the Requirements
for the Degree of
Master of Science (Biology)

at Concordia University
Montreal, Quebec, Canada

March 2022

CONCORDIA UNIVERSITY

SCHOOL OF GRADUATE STUDIES

This is to certify that the thesis prepared

By: Alaa Selim

Entitled: "FRSH: A Frugal and Rapid bioSensor for in-House use to assess meat spoilage"

and submitted in partial fulfillment of the requirements for the degree of

Master of Science (Biology)

complies with the regulations of the University and meets the accepted standards with respect to originality and quality.

Signed by the final examining committee:

_____ External to Program
Dr. Sana Jahanshahi Anbuhi

_____Examiner
Dr. Malcolm Whiteway

_____Examiner (Chair)
Dr. Aashiq Kachroo

_____Thesis Supervisor
Dr. Steve Shih

Approved by _____
Dr. Robert Weladji, Graduate Program Director

_____2022 _____
`
Dr. Pascale Sicotte
Dean of Faculty

Abstract

FRSH: A Frugal and Rapid bioSensor for in-House use to assess meat spoilage

Alaa Sarah Selim

Biogenic amines (BAs) represent a toxicological risk in many food products. Putrescine is the most common BAs found in food and is frequently used as a marker for food quality. Today there is a lack of regulation concerning safe putrescine limits in food as well as outdated food handling practices leading to unnecessary putrescine intake. Conventional methods used to evaluate BAs in food are generally time and resource heavy, limiting the options for on-site analysis. In this work, we developed a transcription-factor based biosensor for quantification of putrescine, one of the BAs in meat products, using a naturally occurring putrescine responsive repressor-operator pair (PuuR-*puuO*) from *Escherichia coli*. Moreover, we demonstrate the use of the putrescine biosensor with a paper-based cell-free device that enables low-cost and rapid putrescine detection. The system was validated using a variety of consumer meat samples with comparable performance to standard well-plate analysis methods. We propose that our system is ready for use to assess the safety of meat products will contribute to a new phase of low-cost biosensors designed for food safety.

Acknowledgements

First and foremost, I would like to thank Dr. Steve Shih giving me an extraordinary and rare opportunity to be a part of his Lab. It is hard to find a PI that treats their lab as an extension of their family. You gave us the opportunity to grow, develop, and master our craft. You cultured and environment where we could make mistakes and learn from them to be a better scientist not just in biology but also in chemistry, physics, engineering, and many more fields. You took time to learn about who we are beyond the lab, you recognized we were not one-dimensional characters. Thank you for all of your continued guidance and support over these past years. And I will forever cherish my time here, I will be leaving this lab not just a better scientist but also a better person.

I would like to give a special thanks Dr. Kachroo and Dr. Whiteway for taking the time to be a part of my committee. It is their support and belief in me during my first committee meeting that pushed me to excel and focus on my achievements. And for that I am more than grateful for their patience and encouragement.

I would like to thank the Center for Applied Synthetic biology (CASB) that created an environment that supports the exchange of ideas, sustains innovation, and breeds excellence among its peers.

Lastly, I would like to thank the lab as a whole, both those who remain and those who have come and gone, during my time here. It was truly a home away from home, where we celebrated your triumphs and supported during our struggles. Thank you to Angela, Jenny-Anne, Chiara, Kenza, and Fatemeh for being inspiring women scientists. Thank you Zy for sharing your love of fashion, abstract and impressionist art, and post-modernist literature. Thank-you Sam for sharing your love for love of cinematography, cooking, and political discourse.

To Laszlo thank you for telling me stories of your time in Europe and abroad, I loved hearing about them. Thank you for taking the time to read through my thesis, I appreciated your help very much and I am very grateful.

To Jay, working with you was a memorable experience, watching you struggle and then succeed brought me great pleasure.

To Zuwin you always brought a smile to my face, you are an exceptional researcher and see a bright future for you, I wish you the best of luck in the rest of your masters and future endeavors.

To Nick, I enjoyed our deep and lengthy discussions and your unique perspectives left me questioning my values at times. You have great character, potential, and vision which will fuel you present and future successes.

All I can say is, I am more than lucky to have you as a friend James M. Perry. Being in the lab with you made it memorable and enjoyable. You have supported me through my success and my failures—and that one time I spilled acid on myself. You challenged me to overcome my limits, to master my skills, and to learn new ones. You made me feel comfortable to share my passions and accepted my quirks. You always impressed me with your resilience, innovative mindset, leadership, and your ability to communicate complex ideas in the simplest of terms. I will forever miss our coffee breaks, your music, your lab-dances, all your jokes, and stories.

I would like to extend a special thank you to Mohammed Nasr, for being an exceptional colleague. Who guided, encouraged, mentored, and supported me throughout my troubles. You helped me develop the critical skills to conduct exceptional work, develop an eye for detail, and deconstruct experimental failures to narrow down the solution. Working by your side was an incredible experience an

Dedications

I would like to thank my mother and father for all of their sacrifices, their wisdom, their tenderness, their unconditional love, their strength, their prayers, and their charity. They supported me through all of my trials and tribulations, they celebrated my successes, they nourished my curiosity, fired my passions, and guided me through the jungle of life. They raised me, fed me, vaccinated me, and tolerated me through my teenage years to which I dedicate, with reverence, this simple thesis.

To my sister and brother who make laugh and humble me every day.

To my friends I made along the way, thank you for supporting me, making beautiful memories with me, and keeping me sane during my masters.

To Danny Devito for producing and directing “Matilda”. It was this film which ignited a passion to read, be curious, and be a strong independent woman!

Overview of Chapters

This thesis describes the project I conducted over the course of my Master's in Science in Dr. Steve Shih's research group at Concordia University. In this work we were able to design and build a cell-free transcription factor biosensor to detect a small molecular analyte putrescine, from meat samples. This thesis begins with a short overview explaining the theory behind biosensing technology, the different types of biosensors, their applications, and their advantages and disadvantages. We address the challenges posed by these different biosensing technologies by proposing a biosensor that uses transcription factor-based biosensing using cell-free technology. We outline our intent for the biosensor by focusing our efforts to detect putrescine, a biogenic amine that is produced as a result of microbial activity. Which is a consequence of a lack of regulation and outdated food handling practices, resulting in an increased consumption of putrescine which can cause adverse physiological effects.

Chapter 1 The chapter introduces the concept of biosensor technology, with an emphasis on transcription factor-based biosensors and cell-free technology, as this applies for the development of analytical devices for the detection of molecules of interest [putrescine]. This ends with a brief overview explaining the biogenic amine putrescine its relation to food quality [freshness] and how increased consumption can lead to adverse physiological effects.

Chapter 2 Describes the materials and methods for research. It contains detailed accounts of the experimental protocols, validation methods, and the data analysis for the results presented in chapter 3 of this document.

Chapter 3 discusses results in characterizing and validating the putrescine responsive transcription-factor biosensor in a cell-free system. I will describe the synthetic promoter design and construction, the characterization transcription-factor biosensor. As a proof-of-concept transcription factor-based biosensor will be validated with-in a cell free system with meat samples stored at different storage conditions. Lastly, the putrescine biosensor will be affixed to a paper matrix will be further validated by testing with different meat samples stored at different storage conditions.

Chapter 4 presents concluding commentary concerning my work and a future perspective of putrescine-biosensor.

Author Contributions

All Methodology, Validation, Formal analysis, investigation, writing – review & editing, and visualization was done by Alaa S. Selim. Conceptualization, investigation, reviewing and editing of manuscript was done by James M. Perry and Mohammed A. Naser. Review, editing, and paper-device optimization and conceptualizing was done by Jay M. Pimprikar. Conceptualization, formal analysis, writing – review & editing, supervision, project administration, and funding acquisition was performed by Steve C.C. Shih

Table of Contents

List of Figures

List of Tables

List of Equations

List of Abbreviations

BA	Biogenic amines
CFPS	Cell free protein synthesis
eGFP	Enhanced green fluorescent protein
LOD	Limit of detection
LB	Lysogeny broth
PCR	Polymerase chain reaction
TF	Transcription factor
WCB	Whole cell biosensor

Chapter 1: Introduction

In this chapter I will introduce the topic of genetically modified bacterial biosensors; how they function and their applications. I will also introduce ways genetically modified bacterial biosensors are being improved with the use of cell-free technology.

1.1 What is a biosensor?

A biosensor is composed of a biomolecule usually an antibody, DNA, RNA, or enzyme that interacts with a target analyte which generates a signal[1]. As you can imagine biosensors have been used in a number of fields, specifically the food industry[2, 3], medical field[4], and environmental sector[5] to name a few. Biosensors provide better stability, sensitivity, and rapid responses in comparison with lengthy and costly traditional methods.[4, 6]

A simple biosensors requires an analyte of interest, a bioreceptor, and their eventual interaction is termed a biorecognition event resulting in a signal output in the form of light, color, or pH change.[4, 6] A great example of a simple biosensor includes the earliest form of a pregnancy test from ancient Egypt **Figure 1.1A**.[7] Where women would urinate on barley or wheat seeds, if the seed sprouted this indicated that the woman was indeed pregnant. While primitive, several modern studies have indicated that this simple biosensor is 70% effective in identifying pregnancies.[7] In the 1970s Drs.Vaitukaitis, Braunstein, and Ross engineered an antibody that was highly specific towards human chorionic gonadotropin (hCG) and surprisingly enough also sheep blood.[8] They designed a binary test to determine pregnancy; they would mix sheep blood coated in hCG, hCG specific antibody, and the patients urine. If she *was not* pregnant the hCG specific antibodies would bind to the sheep blood and result in clotting. If she *was* pregnant, the hCG specific antibodies would bind the hCG in the urine as well as the sheep blood, resulting in minimal

to no blood clotting **Figure 1.1B**.[9] This improved the quality, accuracy, and response time of pregnancy tests.[9] However, the impracticality of these biosensors where long response time and could only be conducted at the doctor's office. It was only in the late 1980's that immobilized hCG specific antibodies onto paper devices, allowed for rapid at home diagnostic testing—that we are so familiar with today **Figure 1.1 C**.

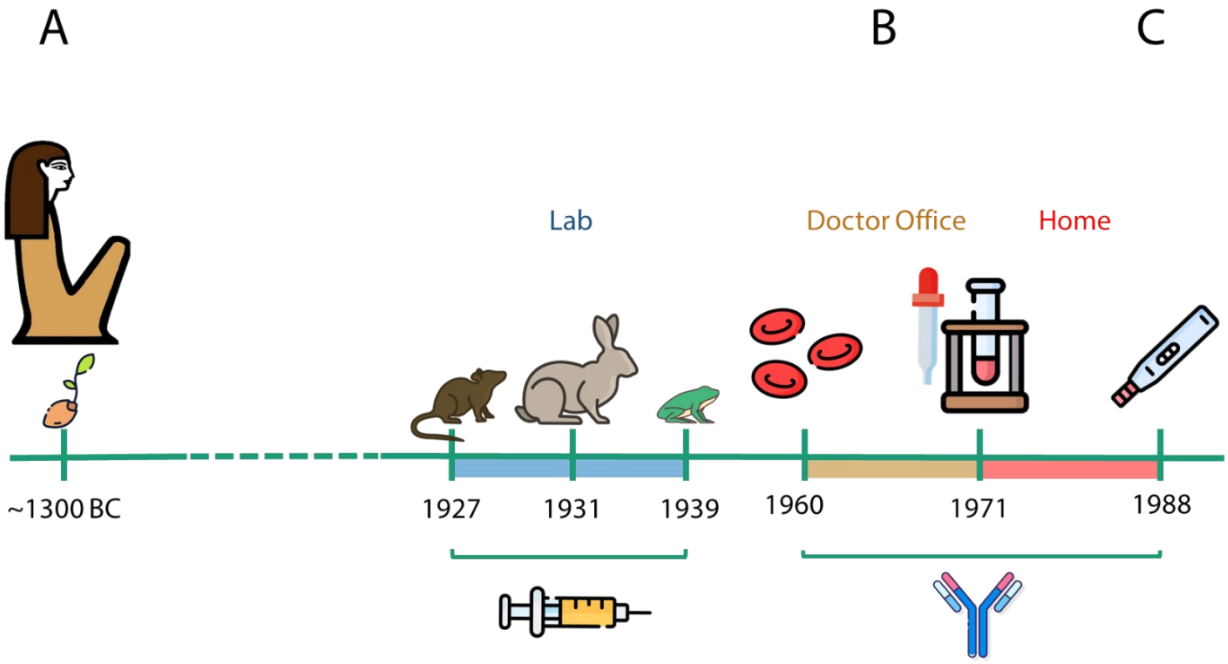

Figure 1.1 – Evolution of pregnancy biosensor. (A) Ancient Egyptian form of a pregnancy test, women who suspected they were pregnant would pee on a barley seed. If the seed germinated, then the where was a 70% chance the woman was pregnant. (B) Advances in antibody technology led to the development of rapid pregnancy tests that where typically performed at doctor offices. (C)Immobilization of antibodies onto a paper microfluidic device allowed for rapid at home testing—no longer requiring lengthy doctor appointments.

1.2 Why Biosensors?

The recent Covid-19 pandemic has emphasized the need for increased testing and has catapulted rapid diagnostics to the fore front of many national and international debates. Coupled with the recent trend toward integrated and automated instruments, biosensors have become a tool for rapid and sensitive tests with which diagnostic measurements can be made.[5, 10] Biosensors are used to detect and determine the relative concentrations of specific analytes in a sample. This basic

principle offers a powerful opportunity[11] for disease monitoring, drug discovery, detection of pollutants, disease-causing micro-organisms and markers that are indicators of a disease in bodily fluids (blood, urine, saliva, sweat).

The appeal of a biosensor lies in its ability to translate the absolute concentration of an analyte in a sample into a measurable signal, therefore providing an avenue of communication.[12] Whole cell biosensors achieve this by controlling the metabolic state of the host, to transduce the target-analyte concentration by modulating gene expression.[13] The reason being is that biosensing technology is ductile, strategic rearrangement of its structure can lead to the detection of a different target analyte(s). This makes biosensors a versatile tool for a diversity of applications for analysis and monitoring of medical, environmental, and industrial relevance. [14]

1.3 Types of biosensors and their applications.

There are many different types of biosensors with a main difference focused on the bioreceptor component. A large repertoire of biorecognition element allows for the development of biosensors for specific conditions and circumstances. Here we discuss the different types of biorecognition components; enzymatic, immunosensors (antibodies), whole cells, genetic, and transcription-factor based and highlight their advantages and disadvantages **Table 1.1.**

Table 1.1: Different bioreceptors used for biosensing technology and their advantages and disadvantages.

Biorecognition Element	Advantages	Disadvantages	Example Applications
Enzymes	**High sensitivity Portability Rapid Response**	**Results can be skewed due to changes in pH or temperature.[15, 16] Some enzymes may exhibit promiscuity.[17]**	**Glucose Oxidase, Cholesterol Oxidase Alcohol oxidase**

Antibodies	**High sensitivity, specificity, selectivity, and strong antigen-antibody binding.**	**Partial denaturation can lead to inaccurate results. Immobilization process is not ideal, due to indefinite antibody orientation. [18] Highly complex antibody processing procedure leading to increased cost.**	**Anti-α-hCG /Anti-β-hCG (Pregnancy-test) Covid-19 IgG and IgM (Covid-19 rapid test)[19]**
Whole-Cells	**Increased stability in a fluctuating environment: salt content, temperature, and pH. Cost effective.**	**Low selectivity. Limited by diffusion resulting in a slow reaction. Interfering background noise. Cannot express toxic proteins.**	**Arsenite whole cell biosensor.[20]**
Genetic (DNA/RNA)	**Wide spectrum of applications. Highly specific due to high binding affinity.**	**Lengthy and costly process [SELEX]. Sensitive to pyrimidine specific nucleases which are abundant in biofluids.[21]**	**Environmental monitoring[22] Cancer detection[23]**
Transcription- Factor	**Highly specific and sensitive. Easy to fine tune performance of biosensor. Can be integrated different chassis.**	**Limited by the range of transcription factor promoter pairs available**	**Monitor Fatty-acid production[24]**

Enzymatic: Enzymes are proteins that catalyze chemical reactions but remains unchanged at the end of the reaction. Enzyme(s) that catalyze target analyte(s) in biosensor will release a by-product(s) that are easily detectable. Rapid sensing and easily detectable by products of biorecognition are convenient factors when designing biosensors. However, enzymatic biosensors present many disadvantages such as cost, complicated purification process, loss of activity when enzymes are immobilized on transducer, and performance is heavily influenced by pH and temperature.

Immunosensors: A class of biosensors that uses antibodies to detect target analytes (antigens). They work similarly to solid-phase immunoassays, where antibodies are immobilized onto a transducer and when exposed to an antigen the immunochemical reaction proceeds to completion. The recognition reaction between the antibody and the antigen is translated by the transducer into a signal that is proportional to the concentration of the antigen (target analyte). Immunosensors offers highly specific and sensitive detection coupled with the availability of engineered antibodies to identify a broad range of molecules.[25]

Whole cell biosensors: Cells are known to be sensitive to their surroundings and respond to changes to their environment and different kinds of stimulants. Whole cell biosensors are engineered cells which can be programmed to analyze molecular entities; toxins, carcinogens, and metabolic by products—from the environment and report their cellular concentration in real time.[25] Whole cells are great candidates for biosensing because they harbor a highly evolved regulatory network for tracking changes happening in the external environment.[26] Whole cell biosensors offer a number of advantages making them an attractive component to construct biosensors with. Whole cell biosensors provide information about the concentration of a target analyte in real time and also provide functional knowledge pertaining to the physiological effect of the target analyte on the living cell.[4, 27, 28] Whole cell biosensors are attractive instruments for industrial applications because they communicate information about the effect of a pharmaceutical drug on the cells metabolism, toxicity, and lethality.

Genetic based biosensors (DNA and RNA aptamers): Aptamer based biosensing have gained recent traction in recent years due to its ability to build library of nucleic acid aptamers with varying affinity to the target analyte. Nucleic acid aptamers are selected by an in-vitro selection process called Systematic Evolution of Ligands by EXponential enrichment (SELEX).[29] The process includes incubating the target analyte in a pool of random oligonucleotides, and bound oligonucleotides are separated from unbound oligonucleotides by elution, and finally bound oligonucleotide aptamers are PCR amplified. This process can be repeated multiple times (6-10 times) resulting in increased affinity and specificity towards the target analyte.[30] Another advantage of DNA and RNA aptamers is they can be easily modified with tags, markers, or probes.

Transcription-Factor Biosensor: Nature has developed a regulatory feedback system which include small molecule binding transcriptional factors with a cognate promoter which tightly regulates transcription based on the concentration of small molecule.[31, 32] Currently, regulatory DNA sequences can easily be synthesized and be integrated into a functional synthetic biosensing circuit.

1.4 Transcription-Factor Biosensors

Detection of small single molecules is often lengthy and requires expensive equipment and methods.[3, 4] Biosensors present a cost-effective alternative for small single-molecule detection. There are various types of biosensors such as enzyme-based, immunosensors, DNA biosensors, thermal, and ribozyme biosensors.[4] However, thousands of years of compounded evolution have led to the development of a diversity of small molecule-binding transcriptional regulator proteins and their cognate promoters.[5] Their role is highlighted in prokaryotes, where bacterial transcription factors act as repressors. Therefore, when small (effector) molecules are absent, some transcription factors can bind to operator sequences and effectively stop gene expression. The process of arresting gene expression occurs by mechanically interfering with the binding of the RNA polymerase to DNA **Figure 1.2A**. However, activity of transcription factors is altered when small (effector) molecules are bound to the transcription factor, relieving the operator, and allowing RNA polymerase to bind and facilitate gene expression **Figure 1.2B**. A key example of this system in **Figure 1.2** is the Lac operon.[33]

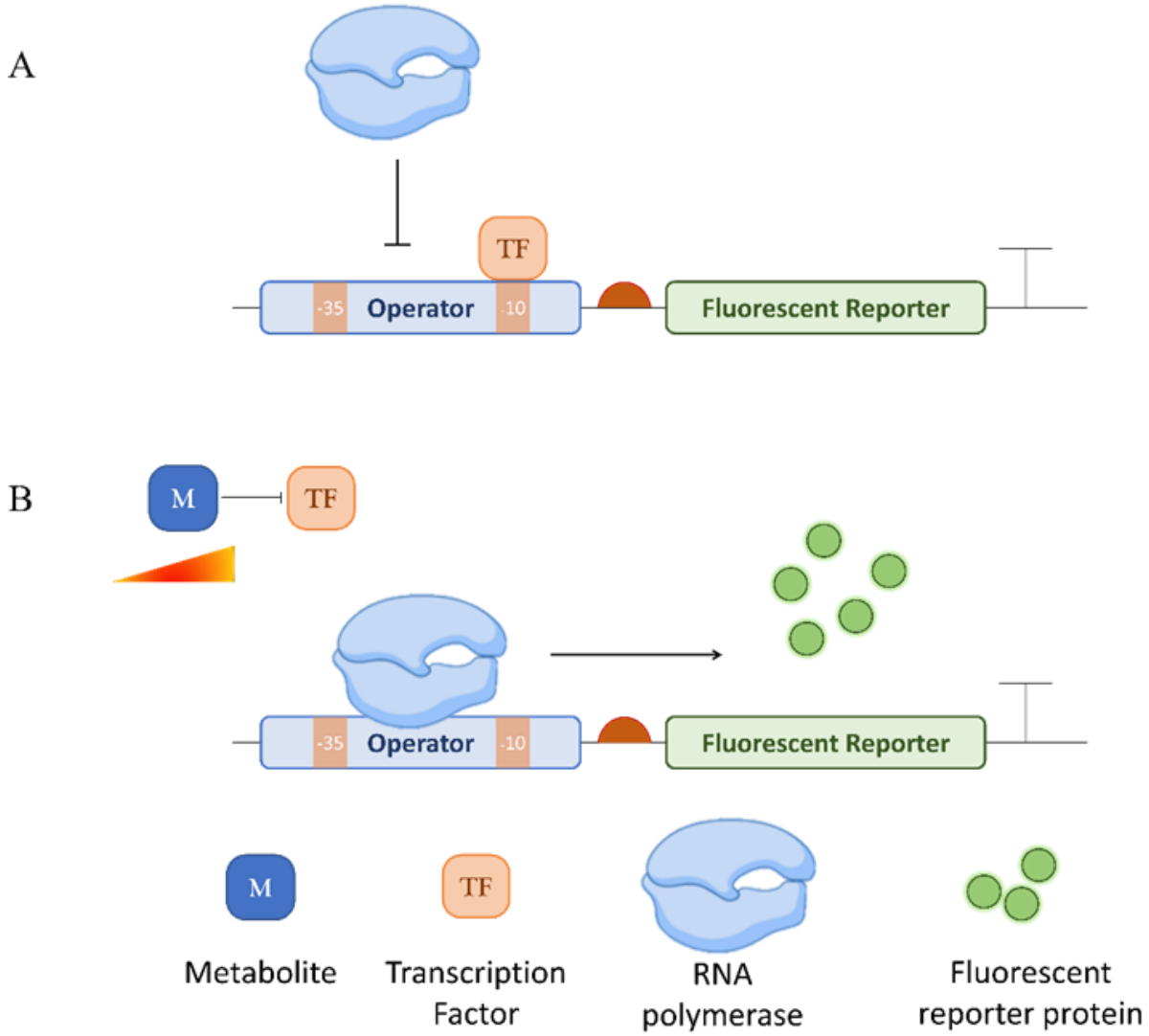

Figure 1.2 – Schematic of a repressor-based TF biosensor in bacteria. (A) In the absence of metabolite of interest, transcription factors will bind to the operator which will effectively repress transcription of the reporter protein, by blocking RNA polymerase. (B) when metabolite of interest is present, metabolite will bind to the repressor protein changing its conformation—making the repressor incapable of binding to the operator, freeing the operator, and allowing RNA polymerase to bind and transcribe the reporter protein.

The ability to manipulate gene expression by modulating metabolite concentration, presents an effective biological switch for biosensing. Therefore using genetic engineering, a transcription factor for a specific analyte can be coupled with a reporter gene (i.e. fluorescent protein or luciferase) to monitor the presence of small molecular analytes[34]. Several studies have successfully

demonstrated the versality of transcription factor biosensors for the detection of arsenic[20], cocaine[35], and fluoride[5]. The robust nature of transcription factor biosensors distinguishes them from alternative bioreceptors like riboswitches and RNA aptamers. The flexible three-dimensional structures of riboswitches and RNA aptamers is a point of vulnerability, they are incredible susceptible to changes in pH and ionic strength making them a difficult to work with.

Presently a myriad of naturally occurring TF regulatory networks exist to monitor small molecular analytes, in order to maintain homeostasis within a living cell. However, these regulatory systems can be in fashioned into a synthetic biosensor(s) to indicate the presence of; small molecular analyte(s),[36] pH change,[37] temperature fluctuations,[38] and much more. Simple molecular methods (i.e cloning) enable biologists to fine tune the biosensor parameters making them easily adaptable for commercial use. A great example of a synthetic biosensor is the ROSALIND system, which uses TF's and their complementary synthetic DNA transcription templates in a cell free system to detect analyte(s) of interest in contaminated water samples.[39]

1.5 Cell Free Biosensors

Recently there has been an increase in the development of whole-cell biosensors (WCB) for a number of applications: clinical-diagnostics, water quality management, food quality and much more.[40] However, their efficiency has been held-back by intrinsic limitations of microbial cells, resulting in reduced sensitivity, selectivity, limited detection range, and response time. The main challenges that affect their efficiency are: maintaining the cells viability, membrane transport, and cell viability when sensing toxic compounds.[39] Another challenge is the time-consuming process of culturing cells to determine the presence or absence of a target analyte in a sample is impractical in the context of today's fast-paced society or field deployment.[41] However, a number of recent

studies have been conducted using cell-free protein synthesis (CFPS) as an alternative tool, mainly due to the fact it addresses the many limitations proposed by WCB's.

The emergence of CFPS as a simple, rapid, and scalable alternative has resulted in a significant departure from cell-based protein synthesis.[42-44] CFPS is an attractive system because of its reductionist composition; it is devoid of its membrane boundaries and contains the components necessary for protein synthesis.[40] CFPS effectively decouples the cell's objectives [growth and reproduction] from the engineer's objectives [protein expression]; the systems resources and energy will be funneled towards over expression of the protein of interest.[45] CFPS has the capacity to prioritize the engineer's objectives and has expanded its use becoming a transformative tool for applications in synthetic biology. It achieves this by facilitating a simplified organization of complex experiments, making CFPS a powerful tool in biological research.[40]

The CFPS system is a mix of DNA template, transcriptional machinery, translational machinery, necessary substrates (amino acids, high energy molecules, cofactors, and salts), and water to properly execute protein synthesis **Figure 1.3**. When these components are mixed and incubated, the machinery can transcribe the DNA template into mRNA and the translational machinery is able to synthesize the protein from the mRNA template. This system facilitates the integration of more intricate genetic circuits and opens up the possibility of complex biosensing functions. This requires the integration of two modules: (1) a recognition mechanism to identify the target analyte and (2) reporter gene which can produced a readable output.[46]

To develop a simple, reliable, and cost-effective biosensor with a high application potential, we coupled a transcription factor-based biosensor with CFPS. Prokaryotic (TF) are proteins that bind to specific genes and regulate gene expression typically by blocking RNA-polymerase and interfering with gene transcription. The ability of transcription factor to bind to specific genes is governed by the presence of specific small (effector) molecules.[47] When these analytes bind to a transcription factor, they inactivate the repressors ability to bind to specific genes allowing for gene transcription to occur. This simple biosensing mechanism can be easily transferred to a cell free system, due to the open nature—the absence of a membrane—of CFPS samples can be readily added to the system and immediately analyzed of reporter gene expression.

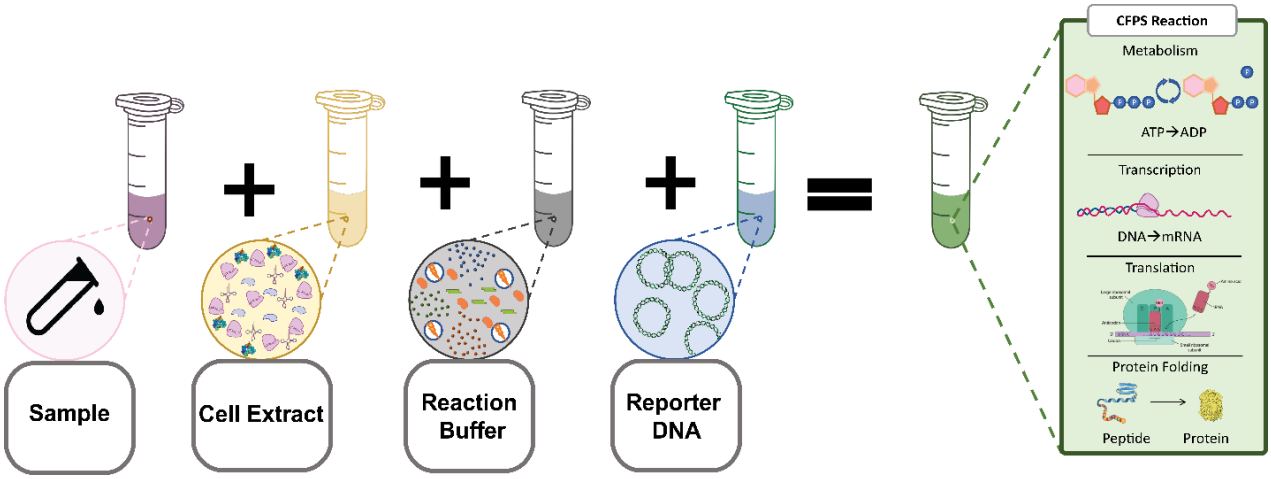

Figure 1.3 – Cell-free biosensor mechanism. Cell-free reaction is composed of four components; cell-extract (with TX-TL machinery), reaction buffer: containing energy, cofactors, and amino acids, reporter plasmid with cognate promoter and reporter gene (i.e., eGFP), and sample with analyte of cell-free reactions are incubated at 37°C for 6 hrs and fluorescent output is measured using a plate reader.

1.6 Analytes of biological interest: Biogenic Amine Putrescine

Biogenic amines are organic, basic, nitrogenous compounds of low molecular weight. Biogenic amines found in nature are typically the result of bacterial metabolic activity, amines in nature are converted by enzymatic decarboxylation into biogenic amines.[48] One example of a biogenic amine is 1,4-diaminobutane often referred to as putrescine, it is used as a monomer for

many industrial applications such as polymers, pharmaceuticals, cosmetics, agrochemicals, surfactants, and other additives **Figure 1.4**.[49]

Putrescine functions as a powerful chemosensory agent, when animals die and begin to rot, they release a disagreeable odor. A pungent component of this scent is emitted by putrescine, which results from the breakdown of fatty acids in the putrefying tissue of dead bodies[50]. Putrescine is an indicator of purification and is described as the smell of death, it constitutes an important signal related to risk avoidance, social cues, and feeding behaviors which are pivotal for surviving.[51] It is well documented that different scavenging insects like Diptera (i.e., flies) and Coleoptera (i.e., beetles), are attracted and colonize a carcass in a relatively predictable sequence called the entomofaunal succession each associated with each stage of decay.[52] Not only is putrescine a metabolite that documents the process of death in cadavers, but it is also a public health concern according to the Food and Drug Administration (FDA) and the European Food Safety Authority (EFSA).[48] Investigating the health implications of putrescine indigestion from food and beverage sources at different stages of decay is a public health concern. Clinical studies investigating the human response to putrescine doses and their toxic effects are scarce. However, one study used real-time cell analysis to investigate the effect of cytotoxic effects of putrescine towards HT29 intestinal cells with concentrations that can be reached by inherently amine rich foods. The IC_{50} value for putrescine was determined to be 39.76 ± 4.83 mM resulting in changes in intestinal cell morphology and eventual deterioration due to necrosis.[53] This is the most recent

comprehensive study that investigated the effects of putrescine to human physiology at the molecular level.

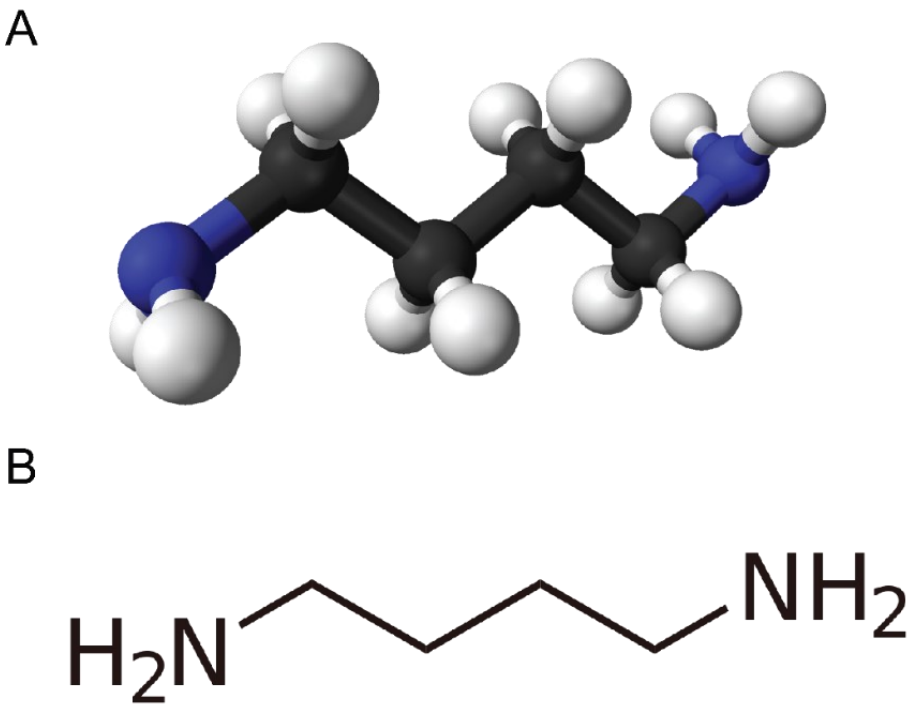

Figure 1.4 – Putrescine chemical structure (A) Ball-and-Stick and (B) Lewis structure of the biogenic amine putrescine.

1.7 Putrescine and Food Quality

A characteristic of globalization and a growing world population is a demand for a sustainable food supply. Since the 1950's there has been a growing trend of importing food from abroad; in fact, it is most likely that the food on your plate has traveled a longer distance than you did bringing it home from the shops. In every stage of the food processing chain, there is a risk of food contamination of different origins: bacteria, viruses, parasites, mold, contaminants, and in some cases chemicals or natural toxins.[54] In addition, the environmental factors like temperature, pH, and salt content in which food is stored can propagate microbial contamination.[55]

This indicates that there needs to be a system that can identify food safety hazards at an early stage so they can be addressed in time before developing into a real public health risk.[56] As a result, food safety has been a topic of public health legislation, and regulations are published to prevent and mitigate these hazards based on their characteristics and behavior. For example, good practices for agriculture and manufacturing (i.e. good agricultural practice (GAP)), as well as the hazard analysis critical control points (HACCP) are a set of guidelines to assess risks and control them.[57] The FDA has published their own guidelines for food freshness assessment. The FDA has defined food decomposition as "the bacterial breakdown of the normal product tissues and the subsequent enzyme-induced chemical changes. These changes are manifested by abnormal odors, taste, texture, color and so on."[58] No chemical analysis are used or proposed instead visual and sensory analysis of these changes are monitored to detect, grade, and confirm the degree of decomposition based on a PASS-FAIL system. Yet it can be envisioned that for several risks, such measures may not be applicable given that these risks are yet unknown or unanticipated. One such unanticipated food toxin or contaminate is putrescine, a volatile biogenic amine, which is formed in food and beverages as a result of microbial action during the aging and storage process.[59]

In addition to the toxic effects, the occurrence of putrescine in food leads to organoleptic properties and adversely affects the appearance, taste, and aroma of food.[60] Biogenic amines are found in virtually all food products composed of proteins or free amines; however favorable conditions will permit uncontrolled exponential microbial enzymatic activity.[59, 61] Bacterial species like *Enterobacteriaceae, Clostridium, Lactobacillus, Streptococcus, Micrococcus,* and *Pseudomonas* have the capacity to decarboxylate amino acids.[54] During the decomposition process, free amino acids are released due to proteolysis, these free amino acids are a nitrogenous energy source for bacteria.[54, 55, 62] The bacterial uptake of free amines is enzymatically processed

by amino acid decarboxylation which results in the synthesis of biogenic amines in food **Figure 1.5**. Amino acid decarboxylation is not found in all bacterial species, however bacteria that evolved to decarboxylate amino acids can adapt to an environment rich in free amines. Biogenic amines for bacteria are an energy source, provide resistance to acidic environments, regulate DNA expression, and act as antioxidants—contributing to their adaptabilities. [63]

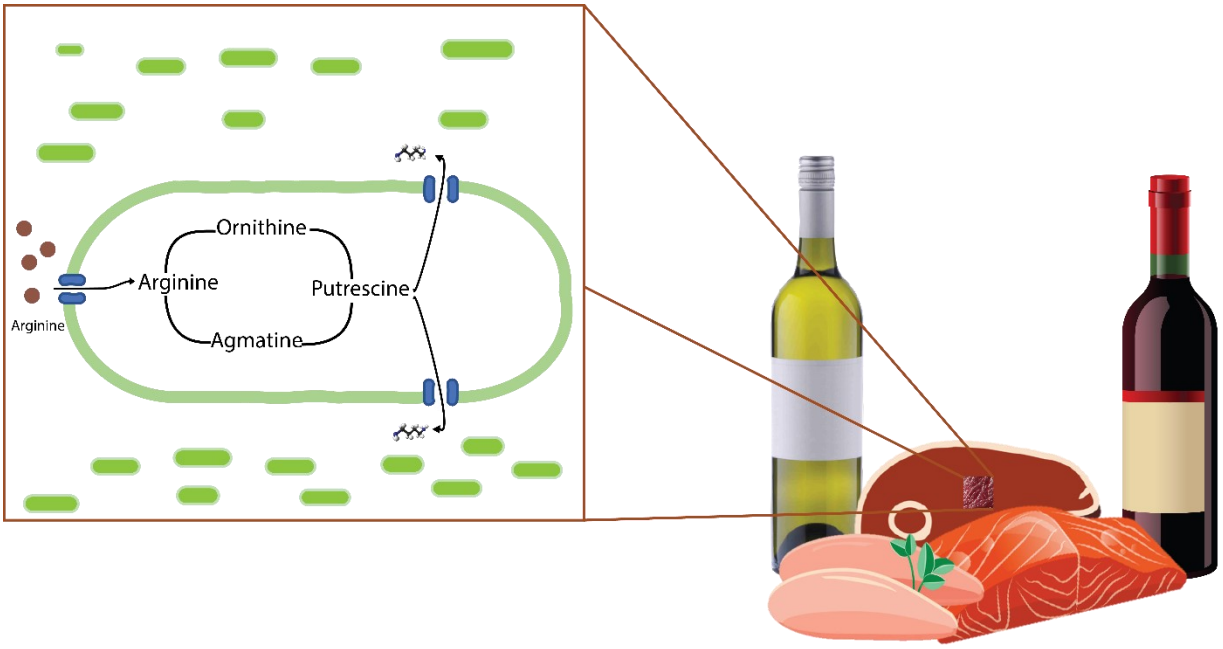

Figure 1.5 – Putrescine accumulation in food products. Putrescine synthesis is propagated by arginine uptake as an energy source. The Arginine is then converted to putrescine via metabolic pathway catalyzed by a decarboxylase enzyme.

Therefore, biogenic amines could be used as an indicator of poor quality or of poor manufacturing practices.[55] Biogenic amine detection is an important indicator of food quality because food appearance is not a relevant feature of freshness, in fact, food that appeared unspoiled could still indicate a high concentration of biogenic amines.[55, 64, 65] A high occurrence

of putrescine in food correlates to microbial activity which is a strong indicator for spoilage in food products. The concentration of putrescine, histamine, and cadaverine represents the freshness of food and is defined in a mathematical formula to calculate the biogenic amines index (BAI) or quality index (QI).[66]

$$BAI = \frac{histamine\left(\frac{mg}{kg}\right) + putrescine\left(\frac{mg}{kg}\right) + cadaverine(\frac{mg}{kg})}{1 + spermadine(\frac{mg}{kg})apermadine(\frac{mg}{kg})} \quad (1.1)$$

When the BAI or QI is calculated, the evaluation can be used to determine the freshness of the food product(s) **Table 1.2**.[67]

Table 1.2: Biogenic Amine Index can be used to determine the quality of meat.

Biogenic Amine Index (BAI)	Quality Evaluation
BAI≤5	High-quality fresh meat
5≤BAI≤20	Meat with acceptable quality with initial signs of spoilage.
20≤BAI≤50	Meat is of low quality
BAI>50	Meat is spoiled

1.8 Physiological effects of putrescine

Here we will investigate what role putrescine plays on the physiological level, and how a rise in putrescine concentration can affect our physiological systems. There are three sources of putrescine within the human body, from which putrescine can bioaccumulate: healthy cells can biosynthesize putrescine for regulatory functions, the intestines can house bacteria that produce putrescine, and direct consumption of food products.[68]

Studies have shown that putrescine rapidly distributes within the body and is easily absorbed, this was evidenced by using *ex-vivo* rat models in which 70% of ^{14}C-putrescine administered was found in the portal vein, 10 min after administration.[69] The result from the study indicates that putrescine is a vasoactive amine, consequently increasing cardiac output, heart

failure, cerebral hemorrhage, as well as tachycardia, or hypotension.[68] The toxicological effect of putrescine is low; however, its secondary effects have a serious impact. Putrescine can enhance and potentiate the toxicological effects of other BA like histamine and tyramine by interacting with enzymes that metabolize these BAs.

The human body is an endogenous source of biogenic amines, and for good reason, polyamines are necessary for many biological functions like cell proliferation, differentiation, modulation of gene expression, apoptosis, and neurotransmission.[70] However, disrupting the homeostatic levels due to increased intake of putrescine from food can have serious toxicological effects. Their molecular characteristics contributes to their necessity for cell physiology, they can easily bind to polyanionic molecules like DNA, RNA, and phospholipids.[71] Under physiological pH and ionic strength conditions—much like physiochemical environment of a cell, biogenic amines are protonated at both termini.[72] Putrescines' amine groups will interact with the phosphate groups in the minor groove of the DNA molecule affecting its stability.[73] In addition to DNA, putrescines protonated termini will interact with other negatively charged molecules such as RNA, phospholipids, and certain proteins. These purposeful molecular interactions result in regulatory structures which can modulate gene expression at different levels including transcription and amino acid translation.[74] The interruption and deregulation of these complex regulatory mechanisms is involved in the manifestation of illnesses like cancer, neurodegenerative disorders, and cytotoxicity.[75]

A serious aspect of putrescine is its ability to form carcinogenic nitrosamines by reacting with nitrates (NO_2^-), a common food additive. The reaction results in the synthesis of N-nitrosopyrrolidine a Group 2B carcinogen (possible human carcinogen) as classified by the Intl. Agency for Research on Cancer (IARC). Biogenic amines are necessary for cell growth,

proliferation, and differentiation by regulating gene expression and enzymatic activity. An increased amount of putrescine intake can result in an imbalance which would affect process like cell growth and proliferation. Multiple studies have observed elevated levels of biogenic amines in cancer cells including blood and urine of cancer patients.[76, 77] Elevated levels of biogenic amines have been associated with tumorogensis.

Bioaccumulation of putrescine will disrupt physiological balance and effect functions of cell differentiation, proliferation, and regulation. As a result, elevated levels of putrescine intake can have serious short term or long-term effects on an individual either by increasing the toxic potency of other biogenic amines (histamine or tyramine) or reacting with nitrates to form N-nitrosopyrrolidine, a Group 2B carcinogen. Because putrescine plays a critical role in maintaining physiological balance and is rapidly absorbed by the body, monitoring alimentary intake becomes a necessity to avoid cytotoxic effects. Biogenic amines play a large role in the physiology of tissues that are characterized by high rates of cell division such as the lumen of the digestive tract—making them vulnerable to tumorigenesis.[71]

1.9 Thesis objectives

To address the challenges posed by current putrescine biosensors, we introduce a rapid and portable paper device to detect the putrescine content in protein-rich foods (e.g., meats). FRSH a novel biosensor that combines cell-free technology with transcription-factor based biosensing to make a frugal and rapid biosensor for in-house use to determine the quality of meat which may have been subject to unhygienic practices. This work will highlight the biosensors central advantages which are a (1) rapid and portable biosensing device (2) high specificity towards putrescine, as BA are usually the first compounds to be released during the decomposition of meat and (3) A limit of detection (LOD) below a defined limit of 39.76 ± 4.83 mM, which when applied

to intestinal cell (HT29) cultures results in cell necrosis.[53] To achieve this, my research was divided into these following objectives:

1. Design and build a TF biosensor: Using a naturally occurring putrescine responsive transcription factor PuuR, we designed and built a modified library of synthetic cognate promoters by inserting recognized binding regions with-in and downstream the -35 and -10 site. Furthermore, we characterized the synthetic promoter library in terms of dynamic range, LOD, sensitivity, and specificity to isolate the best performing synthetic promoter.
2. Integrate biosensor into an optimized cell-free system: We sought to leverage the advantages of cell-free biosensing platforms to create a new approach for monitoring for the presence of putrescine. Therefore, we optimized a cost-effective cell-free system which was then used to evaluate the putrescine responsive TF-biosensor and decrease overall response time when tested with meat samples.
3. Proof-of-concept: A paper-device was designed and fabricated to ensure a portable, easy-to-use, and economic alternative to expensive equipment traditionally used to detect putrescine. Cell-free system with TF biosensor was lyophilized onto the paper device and was re-hydrated with meat samples to evaluate biosensor within the context of a field application.

Our work with TF-biosensors in cell-free systems exemplifies its potential as a pragmatic tool for the development of biosensing systems for rapid, cost-effective, easy-to-use, and field deployable diagnostic tool to address spoilage in protein-rich foods [meat]

Chapter 2: Materials and Methods

In this chapter I will describe the methodology for designing and building our synthetic promoter library, the process of characterization of our synthetic promoter library, development, and optimization of our cell-free system for the integration of our putrescine biosensor, and the design and fabrication of our paper device, and meat sample preparation and evaluation.

2.1 *Escherichia coli* strains, primers, plasmids, and reagents

All general-use reagents were purchased from Sigma, unless specified otherwise. Strains and plasmids were described in **Table S1**. Briefly, host strain *E. coli* DH5α and One Shot® BL21 Star™ were obtained from Invitrogen Corporation (Carlsbad, CA, USA). Competent DH5α and One Shot® BL21 Star™ were prepared using Hanahan method.[78] Unless otherwise stated, cells were cultured in lysogeny broth (LB) medium or M9 minimal media, with appropriate antibiotics (kanamycin, carbenicillin, or chloramphenicol at 50, 100, 35 μg/ml, respectively). All primers used were commercially synthesized by Biocorp (Montreal, QC, CA). The plasmid pFAB4876 was purchased from Addgene (#80649).[79] The plasmid pTU1 was obtained from the EcoFlex MoClo kit purchased from Addgene (#1000000080). Phusion® high-fidelity DNA polymerase, Taq DNA polymerase, T4 DNA ligase, DpnI, and BasI-HF® were purchased from New England Biolabs (Ipswich, MA, USA). Invitrogen PCR purification kit, Biobasic gel extraction kit, and Biobasic miniprep kit were purchased from Cedarlane (Ontario, Canada).

2.2 Construction of the putrescine biosensor: repressor and reporter plasmids

The putrescine biosensor contains a dual plasmid system consisting of a repressor (which we call 'PuuR') and a reporter plasmid. As shown in **Figure S1**, the repressor plasmid exclusively used parts from the Ecoflex MoClo kit[80] and was constructed using an optimized, one-pot Golden Gate

assembly protocol adopted from previous work.[81] The repressor plasmid contained the modified pFAB back bone (see **Supplemental Protocol S1**), T7 promoter, RBS, His-tag, and terminator (BBa_B0015) genes and the repressor protein PuuR (see **Table S2** for DNA sequences) which was commercially synthesized by Twist Bioscience (San Francisco, CA, USA). For the repressor plasmid assembly, BsaI restriction site were used as the type IIS restriction cut site for Golden Gate assembly. The PuuR DNA insert was PCR amplified by primers PuuR_R and PuuR_F harboring BsaI restriction sites (see **Table S3** primer sequences). Inserting the restriction site was performed in a 50 µL PCR reaction containing 43.5 µL GC master mix (5x G/C buffer, 100% DMSO, 100 mM ATP/TTP/GTP/CTP), 2.5 µL of primer PuuR_R, 2.5 µL of primer PuuR_F, 1.0 µL of PuuR template, and 0.5 µL Phusion® high-fidelity DNA polymerase (NEB) using PCR conditions listed in (**Table S4)**. The PCR reaction of PuuR was then loaded onto a 0.8% agarose gel and purified using BioBasic gel extraction kit according to manufactures instructions. The concentration of the gel purified PuuR was measured using a Tecan Infinite® 200 PRO (Tecan Group Ltd., Switzerland) and was used for the Golden Gate reaction in the next step. To prepare for the assembly reaction, an overnight culture of the vector backbone pFAB was inoculated in LB with kanamycin selection, and isolated following the manufacturer's instructions from the Biobasic miniprep kit. Additionally, T7 promoter, RBS-linker, His-tag, and terminator (BBa_B0015) genes from the pTU1 backbone were obtained from the EcoFlex MoClo kit (Addgene) and were each inoculated with 5 mL of LB media with 35 µg/ml of chloramphenicol selection and cultured overnight at 37°C. Plasmids containing each gene were isolated using the Biobasic miniprep kit. To perform the assembly, 1.5 µL 10× T4 Ligation Buffer, 1 µL BsaI (or BsaI-HF®) (20 units), 1 µL T4 DNA Ligase (1–3 units), 50 ng pFAB destination vector, and 50 ng of each part (T7 promoter, RBS-linker, His-tag, PuuR insert, and terminator (BBa_B0015))

were added into a tube and topped up to 15 µL with ddH_2O and mixed via pipetting up-and-down. The reaction was incubated in the thermal cycler with the following program: 37 °C for 5 min then 16 °C for 10 min—repeated for 30 cycles—with an ending cycle at 50 °C for 5 min and at 80 °C for 5 min. Next, 2.5 µL of the assembly reaction was added to 25 µL DH5α for heat-shock transformation at 42 °C for 45 seconds and recovered in 200 µL SOC media and plated on pre-warmed 50 µg/mL kanamycin agar plates. Five randomly chosen transformants were selected for colony PCR using Taq polymerase in a 50 µL reaction using primers pFAB_frwd and pFAB_rev, reaction was carried out following reagents and thermocycler conditions listed in **(Table S4).** Colonies with positive colony PCR results were inoculated overnight in LB with 50 µg/mL kanamycin. A glycerol stock was made by mixing 1 mL of overnight culture with 1mL of 50 % (v/v) glycerol solution in a cryovial tube and stored for long term storage in -80 °C freezer.

For the reporter plasmid, there were four parts that were assembled in the plasmid backbone – the *puuO* promoters, RBS, eGFP, and the terminator (**Table S2)**. In total, 11 synthetic promoters **(Table S2)** were built using primers by a sowing PCR method to build the library (see **Figure S2** for workflow). To assemble each synthetic promoter, we performed two rounds of PCR: in the first round, the core promoter was amplified by two over lapping primers (primer_2F and primer_2R; **Table S3**). To add flanking BsaI restriction sites to the core promoter, a second round of PCR was performed using primers: primer_R and primer_F. Each PCR reaction contained a 50 µL reaction volume consisting of 0.5 µL Phusion® high-fidelity DNA polymerase (NEB) with 2.5 µL of each primer: primer_2F and primer_2R and the reaction was topped up with 43.5 µL G/C master mix (5x G/C buffer, 100% DMSO, 100 mM ATP/TTP/GTP/CTP). The conditions of the PCR followed **Table S4**. Gel purification of the promoters and overnight inoculations of the pTU1 backbone, RBS, eGFP, and terminator (BBa_B0015) and isolation followed the protocol for the

repressor plasmid except with 35 µg/ml chloramphenicol selection for inoculation. In addition, assembly **(**using Golden Gate **Table S5)**, transformation, and colony PCR protocols followed the protocol for the repressor plasmid. Successful assemblies were inoculated overnight in 5 mL of LB with 100 µg/mL carbenicillin. To make a glycerol stock, 1 mL of overnight culture was mixed with 1 mL of 50% (v/v) glycerol solution in a cryovial tube for long term storage in -80 °C freezer.

Sequential transformation was used to incorporate both the repressor and reporter plasmids into BL21 DE3 *E.coli* for our cell-based sensors. One Shot® BL21 Star™ competent cells were prepared using Hanahan method.[78] To start, 50 µL of BL21 DE3 star™ competent cells were thawed on ice, and 10 ng of repressor plasmid (PuuR) was added to 50 µL of competent cells and gently mixed by up and down pipetting. For the first transformation, the mixture was incubated on ice for 30 min, heat shocked for 30 s at 42 °C, and returned to ice for 5 min. 950 µL of room temperature SOC media was added to reaction tube and incubated in shaking incubator for 1 h at 37 °C. After 1 h, reaction tubes were spun down and 900 µL of LB was removed. The remaining 100 µL was resuspended and spread on pre-warmed agar plates with 50 µg/ml of kanamycin selection and incubated overnight at 37 °C. Five randomly chosen colonies were selected for colony PCR reaction using the same conditions as above. Successful transformants were inoculated overnight in 5 mL of LB with 50 µg/mL kanamycin to make a starter culture for competent cells. The 5 mL starter culture of BL21 DE3 star™ with repressor plasmid was used to prepare chemically competent cells according to the Hanahan method. Next, 50 µL of the competent cells containing the repressor plasmid was used to transform 10 ng of each reporter plasmid and was used for heat shock transformation. After applying 42 °C for 30 s, cells were plated on agar plates with 50 µg/mL of kanamycin and 100 µg/mL carbenicillin. Successful transformants were picked inoculated in LB media with both 50 µg/mL of kanamycin and 100

μg/mL carbenicillin and grown overnight. This was done for the promoter library, and 1 mL of overnight culture was mixed with 1 mL of 50 % (v/v) glycerol solution in a cryovial for long term storage in -80 °C freezer.

2.3 Characterization of the putrescine biosensor

Cell culture and fluorescence detection: In a 96 deep-well plate (Corning Costar 3603, New York, USA), *E. coli* strains carrying the co-transformed promoters were inoculated in 1 mL of M9 minimal media with 50 μg/mL of kanamycin and 100 μg/mL carbenicillin and grown overnight in an orbital shaker (Infors-HT, Bottmingen, Switzerland) at 37 °C at 250 rpm. Cultures were 100-fold diluted into fresh 100 μL of M9 minimal media with above-mentioned selection and incubated at 37 °C at 250 rpm for 3 hours until the optical density reached 0.3 - 0.5. Cultures were induced with 0, 0.1, and 0.5 mM of IPTG and supplemented with putrescine to a final concentration of (0 mM, 0.1 mM, 1 mM, 10 mM, 50 mM, 100 mM, 500 mM, 1000 mM). Additionally, each plate included controls: cells with only repressor plasmid, only BL21 DE3 star™ cells, and only M9 minimal media were also induced with putrescine. After 16 h, at 37 °C with shaking at 250 rpm, optical density at 600 nm (OD_{600}) and GFP fluorescence (excitation at 488 nm and emission at 507 nm, gain of 1900) of each well was measured using a well plate reader (CLARIOstar, BMG Labtech, Germany) using the endpoint option. Fluorescent output was normalized to cell density measured at OD_{600} and background corrected by subtracting the normalized fluorescence of cells lacking eGFP reporter. All putrescine induction reactions were done in triplicates. All data points were represented as an average with error bars displaying standard error of the mean (SEM). Graphs were plotted using GraphPad Prism 9.0 and the fluorescence data was fitted with a Hill function.

Dose-response and sensitivity: To plot a dose-response curve, we followed Mannan *et al.* and Chen *et al.,*[47, 82, 83] which include parameters such as basal expression ($eGFP_{min}$), maximal expression ($eGFP_{max}$), dynamic range (μ), K_A, and response sensitivity defined as the slope of the dose response-curve or the Hill coefficient 'n'.

$$y = eGFP_{min} + \frac{x^n(eGFP_{max} - eGFP_{min})}{(x^n + K_A^n)} \quad (2.1)$$

In Equation 2.1, y represents the normalized fluorescence ($R.F.U/OD_{600}$) in accordance with putrescine concentration at value x. K_A represented the putrescine concentration that induces a response halfway between the baseline and maximum response at a specific putrescine concentration. n is the Hill coefficient which describes sensitivity, the ability to distinguish small differences in putrescine concentrations.[36, 84, 85] $eGFP_{min}$ and $eGFP_{max}$ represent the fluorescence signal from a blank putrescine control with 0.5 mM IPTG and fluorescence signal measured at 16 h, respectively.

Limit of detection: To calculate the limit of detection (LOD) a linear regression was extrapolated from the dose-response curve for all promoters. From the linear regression, the LOD was calculated using Equation 2.2.

$$LOD = \frac{3.3(\sigma)}{S} \quad (2.2)$$

Where σ is standard deviation of the linear range of dose-response curve, and *S* is slope of the linear range of the dose-response curve.[86]

Dynamic range: Dynamic range was evaluated by measuring the fold change in signal output in the presence and absence of the inducer putrescine. Dynamic range (μ) was calculated by dividing normalized fluorescence of $eGFP_{max}$ over $eGFP_{min}$ using Equation (2.3) as a reference.[47]

$$\mu = \frac{eGFP_{max}}{eGFP_{min}} \quad (2.3)$$

Specificity: Specificity testing was performed to determine if the biosensor was promiscuous with other analytes. Biogenic amines with very similar molecular structure and characteristics (e.g., histamine and cadaverine) were exogenously added to the whole cell biosensor (0 mM, 0.1 mM, 1 mM, 10 mM, 50 mM, 100 mM, 500 mM, 1000 mM) and their output fluorescence was measured following our culture protocol above. To quantify TF-biosensors specificity, we calculated the percent increase of the normalized fluorescence of cadaverine, and histamine compared to putrescine at 50 mM (closest value to our target putrescine concentration).

2.4 Cell-free putrescine biosensor system

Cell extract was prepared according to a modified protocol by Levin *et al.*[87] where *E. coli* BL21 DE3 star™ cells were transformed with repressor plasmid expressing the transcription factor PuuR. To harvest, lyse, and to make the cell extract for the cell free biosensor, we followed detailed protocols as described in **Supplemental Protocol S2**. Cell free reactions were prepared by mixing cell lysate (referred to as solution A), reaction buffer (solution B and solution C), and plasmid DNA, putrescine inducer, and water. All cell-free reactions were carried out in 15 µL in 1.5 mL microcentrifuge tubes in triplicates, unless otherwise stated. Generally, three solutions

were prepared to test the biosensor under cell-free conditions: solution A (15 mg/mL of cell lysate as described in **Supplemental Protocol S2**), solution B (1.2 mM ATP, 0.850 mM GTP, 0.850 mM UTP, 0.850 mM CTP, 31.50 µg/mL folinic acid, 170.60 µg/mL tRNA, 0.40 mM nicotinamide adenine dinucleotide (NAD), 0.27 mM coenzyme A (CoA), 4.00 mM oxalic acid, 1.50 mM spermidine, and 57.33 mM HEPES buffer), solution C (2 mM $Mg(Glu)^2$, 10 mM $NH_4(Glu)$, 20 mM K(Glu), 2 mM each of the 20 amino acids, and 0.03 M phosphoenolpyruvate (PEP)). All solutions were thawed on ice for 10-15 min. For calibration curves, 2.1 µL of solution A, 2.2 µL of solution B, 5.0 µL solution C, 50 ng/µL of reporter plasmid, putrescine between 10 mM - 100 mM, and DNase/RNase-free water were mixed together to bring the final reaction volume to 15 µL.

2.5 Paper-disc fabrication and sample loading

Paper disc devices were fabricated according to previously published protocols.[5,88] Essential to our device design was to minimize cross contamination and facilitate quantifying eGFP output using the well-plate reader. With these criteria, we constructed a device with four separate 5 mm disks (9 mm diameter center to center), with the intention of being able to line the devices with the configuration of a Greiner 96 half-bottom well plate. Aluminum foil (Kingsford Extra Wide Aluminum, 25µm), positional mounting adhesive (3M), and cold roll laminator (INTBUYING, Scarborough (ON), Canada) were purchased from Amazon. For the paper substrate, cellulose chromatography Whatman Grade 1 (GE health care, 20 cm x 20 cm x 0.188 mm) was purchased from VWR. Whatman paper was affixed onto the mounting adhesive and gently peeled off, then transferred onto an aluminum sheet and trimmed to paper dimensions (measuring 20 cm x 20 cm). The foil-backed paper was fed through the cold-roll laminator to enable binding and to eliminate

any air bubbles. Using AutoCAD, we designed paper disc devices with four separate loading zones: two discs containing cell-extract with-out the reporter plasmid and two discs containing cell-extract with the reporter plasmid. The discs are 5 mm in diameter and are spaced out from center-to-center at 9 mm. This device pattern was laser engraved using a 60 W CO_2 laser (Trotec Speedy, Trotec, Marchtrenk, Austria) with the following settings: 10% speed, 60% power, 1000 ppi, 35 psi of compressed air.

Individual devices were cut using a tabletop paper cutter (X-ACTO, Westerville (OH), United States) and placed in a glass Petri dish and immersed in 4% BSA solution with 50 mM Tris buffer pH = 7.5 and left to incubate for 1 h. Devices were transferred to a clean petri dish and left to air-dry overnight which was then ready for use. After drying each reservoir was loaded with 5 μL of cell free reaction. Two of the reservoirs were loaded with 5 μL of cell-free reaction without the reporter plasmid, and the other two reservoirs were loaded 5 μL of cell-free reaction with the reporter plasmid. Liquid nitrogen was poured over the paper devices and transferred to lyophilization jar (Fast-Freeze Flask). Paper devices were lyophilized at 0.04 mbar at -50 °C for 12 h. For long term storage, devices were stored in a box with calcium sulfate (Drierite) at room temperature.

2.6 Putrescine biosensor testing with beef samples

To study the bioaccumulation of putrescine in real food samples, beef steak was purchased from a local grocery store. Beef was transported to the lab under ambient conditions from the local supermarket within 30 min. In the lab, beef was transferred to sterile containers and stored at -20 °C. Sterile containers were labeled with the date and supermarket. Using a sterile razor blade, 5.0 g of beef was cut and weighed individually on separate and sterile boats. The meat was transferred

to a 50 mL Falcon tubes and were tightly sealed by wrapping lids with Parafilm and were immediately transferred to -20 °C. To determine the effect of temperature on meat quality, beef samples were subjected to different types of storage commonly used: fridge (4 °C), room temperature (20-22 °C), and frozen (-20 °C). The samples were left under these conditions for 6 days. On day 2 and on day 6, 1.0 g from the sample and 1.0 mL of phosphate buffer solution (PBS) were mixed and vortexed for 1 min to ensure uniform mixing between sample and PBS. A 200 µL of the supernatant was aliquoted into a 1.5 µL centrifuge tube and was used for putrescine measurement. To measure their putrescine content, in a cell-free reaction, 2.1 µL of solution A, 2.2 µL of solution B, 5.0 µL solution C, 50 ng/µL of reporter plasmid P_{hyb}(3A), 1.0 µL of the supernatant from the meat mixture, and DNase/RNase-free water were mixed together to bring the final reaction volume to 15 µL.

Prior to aliquoting on the paper disc device, the meat samples were centrifuged at 10,000 rpm for 2 min to remove any debris. Next, 200 µL of the meat supernatant was aliquoted from the meat samples used in the above mentioned 15 µL cell-free reactions. Paper biosensors were rehydrated by adding 2.0 µL of the meat sample directly onto the paper disc of the device. The device was incubated bench top at room temperature (20-22 °C) until entire device was saturated with sample for 30 seconds to 1 min. Paper biosensors reservoirs were directly aligned with a center of the well and taped onto plate and placed in a plate reader (CLARIOstar). The eGFP fluorescence was measured at l_{ex} = 488 nm, l_{em} = 507 nm, and gain = 1900 for the calibration curve (see **Supporting Information Protocol S3**). These devices were incubated at 30 °C for 1 to 6 hours and fluorescent measurements were pathway adjusted and well-scanned. The amount of putrescine in the meat samples was calculated from the calibration curve for promoter P_{hyb}(3A).

Chapter 3: Results and Discussion

In this section I will discuss our experimental results the synthetic promoter library characterization in terms of dynamic range, LOD, sensitivity, and specificity. The cell-free optimization and evaluation of our biosensor with spiked putrescine samples and real meat samples, and lastly validation work concerning our paper device with lyophilized cell-free biosensor.

3.1 Design of a putrescine biosensor and its variants

We designed and constructed a putrescine sensor consisting of two genetic circuits: (*i*) the repressor and (*ii*) the sensing circuit (**Figure 1A)**. The regulation of these circuits is coordinated through the expression of the PuuR repressor through the T7 promoter, and this will bind to a synthetic putrescine-inducible promoter containing the operator '*puuO*' on the reporter plasmid. When there is low level or absence of putrescine, the repressor [PuuR] will bind to the synthetic promoter and prevent eGFP production by blocking RNA polymerase from binding to *puuO*'. In contrast, when putrescine is present, it will bind to PuuR, releasing it from *puuO*', allowing for RNA polymerase to bind to the promoter to enable eGFP expression.

A

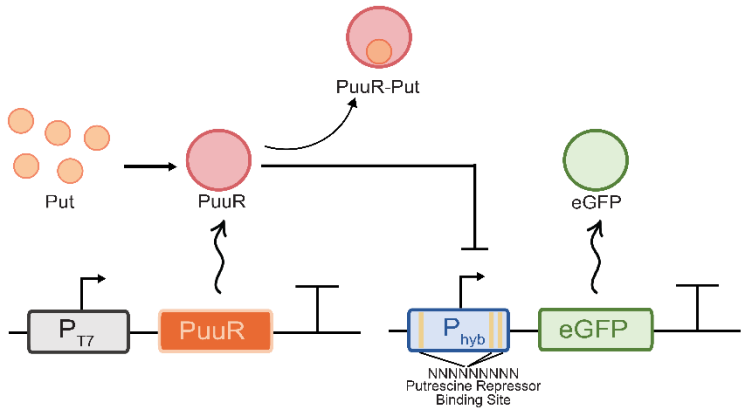

B

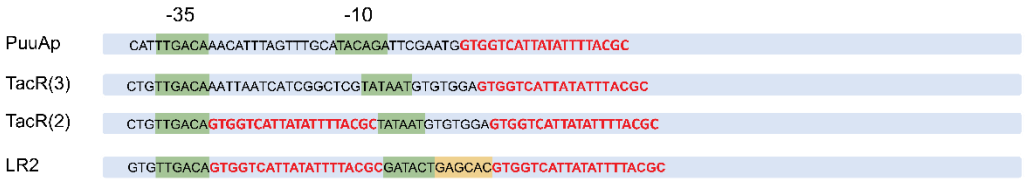

C

$$P_{hyb}=P_{Tac}+P_{LR}$$

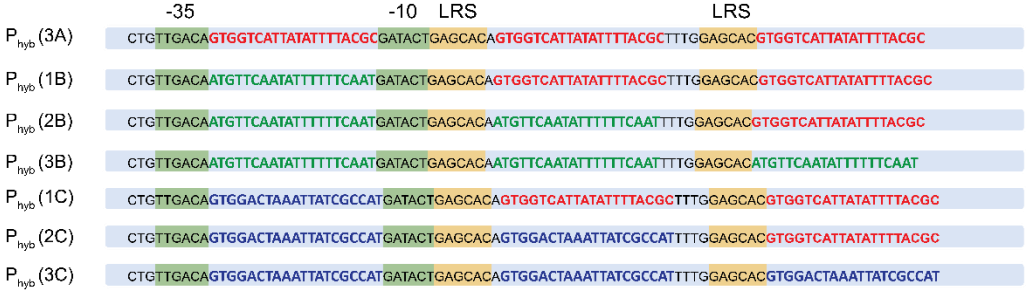

Binding Region	Sequence
A	GTGGTCATTATATTTTACGC
B	ATGTTCAATATTTTTTCAAT
C	GTGGACTAAATTATCGCCAT

D

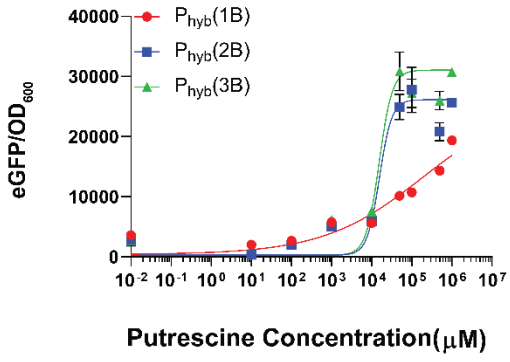

E

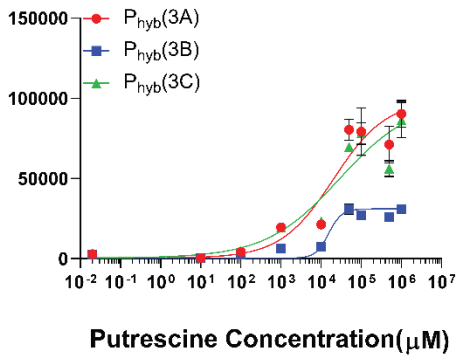

Figure 3.1 – Putrescine biosensor. (A) Schematic of the transcription-factor biosensor for the detection of putrescine. (B) DNA sequence of synthetic promoters PuuAp, TacR(3), TacR(2), and LR2 taken from Chen *et al.*[83] with highlighted red PuuR binding regions, -35/-10 census sequences highlighted in green, and a LR-promoter spacer region highlighted in yellow. (C) DNA sequences of hybrid synthetic promoters ($P_{hyb} = P_{Tac} + P_{LR}$) for this study containing binding regions: A (red), B (green), and/or C (blue) were inserted either within or downstream of the -35 and -10 site. Yellow highlighted areas are LR-promoter spacers. Dose-response semi-log plots based on (D) different placement of the B binding site and (E) type of binding site. Both plots were fitted to a Hill function using Prism. Error bars represent the standard deviation for three replicates.

There have been several reports [83,89] describing the development of synthetic promoters for detecting putrescine. In particular, in Chen *et al*., they modified the Tac (TacR) and the wild-type promoter (PuuAp) to monitor intracellular putrescine production. Tac is a functional hybrid of trp and lac promoters and highly efficient when directing transcription, which can be attributed to the Tac promoter's tight regulation of expression.[90, 91] Furthermore, they showed TacR to exhibit optimal performance and had desirable activity and responsiveness when monitoring intracellular levels of putrescine.[83] Similarly, they also created a phage lambda promoter (LR2) that is also highly active *in vivo,* although it shows 15-30[92] times lower binding affinity for RNA polymerase. Their work is an important step forward for detecting polyamines; however, the main limitation from the study is that their whole-cell biosensor was primarily optimized to monitor endogenous putrescine biosynthesis. Exogenously added putrescine showed very slow response time (> 6 h) and low dynamic range (see quantification below), which can be challenging for meat sample detection.[93] Therefore, to create a biosensor for real meat sample detection, we report new designs of synthetic promoters that can be used for measuring exogenous putrescine from meat samples with faster response times and higher dynamic range.

To engineer our library of synthetic promoters, we used two commonly used strategies: (1) modify the -35 and -10 consensus sequence[94] and (2) add transcription factor binding regions at different locations within the operator[24, 95]. As an initial design, we used the two highest dynamic

range promoters, TacR(2) and LR2 from Chen et al.[83], and generated a hybrid promoter consisting of the "-10" site from the LR2 promoter and the "-35" site from TacR promoter because hybrid promoters are known to be highly efficient when directing transcription compared to non-hybrid promoters.[89, 90] Next, we obtained sequences from *PuuA* and *PuuD* genes,[96, 97] which are known PuuR binding regions: GTGGTCATTATATTTTACGC (we call "A"), ATGTTCAATATTTTTTCAAT (B), and GTGGACTAAATTATCGCCAT (C), and placed these binding regions within (W) and/or downstream (D) of -35 and -10 sites to create different combinations of binding sites as it has been shown that mixing binding sites can lead to changes in the sensing and regulation.[96-98] Using these two strategies, we used 4 promoters from Chen *et al.* as controls **(Figure 1B)** and created 7 hybrid promoters **(Figure 1C)**.

Using our synthetic promoters, we measured the repression dynamics caused by PuuR. In the first step, the promoters were tested in the absence of IPTG (0 mM). We expect without any repression, eGFP to be produced. As shown in **Figure S3**, regardless of the concentration of exogenously added putrescine, the plot confirms that fluorescence is always observed (i.e., no repression is occurring). In contrast, the sensors were interrogated with exogenously added IPTG at concentrations 0.1, and 0.5 mM, to induce PuuR expression. Generally, we observe properties of a sigmoidal curve – sharp increases in fluorescence at higher putrescine concentrations and low fluorescence output at low putrescine concentrations - when the circuit was induced with 0.1 and 0.5 mM IPTG**.** There are two promoters that did not exhibit these biosensing characteristics: TacR(3) and P_{hyb}(1C). TacR(3) shows no repression behaviour while P_{hyb}(1C) shows random fluorescence values for all tested putrescine concentrations. Given the poor characteristics, we eliminated both promoters from our quantification study (see below). Regardless, 6 out of the 7

designed promoters show regulation by induction, with the 0.5 mM induction showing a more dose-like Hill response properties indicating that PuuR is repressing the circuit when it is induced.

Interestingly, we observed differences in the output response when the promoters had different combinations of binding sites. Comparing the output fluorescence levels (at 0.5 mM induction) for P_{hyb}(1B), P_{hyb}(2B), P_{hyb}(3B), they show differences in their fluorescence output. Specifically, the output response for 2B and 3B showed increased sensitivity to putrescine (slopes) and lower response threshold (amount of putrescine for 50 % output expression relative to baseline) **(Figure 1D**) compared to P_{hyb}(1B). Furthermore, we compared the output fluorescence containing the same type of binding site at all three regions. As shown in **Figure 1E,** binding sites A and C show similar dose-response curves but are different when compared to the curve given by B. The major difference is the maximum biosensor output, which is ~2-fold larger for A and C compared to B. We are unsure of the genesis of the differences observed with the combinations of binding sites, but hypothesize that changing the promoter operator site changes the affinity of the transcription factor PuuR to the promoter site.[36, 84, 99] This is observed in other studies[47, 48, 100], where one or two nucleotide changes in the operon can drastically change the overall dose-response dynamics. Indeed, more work is needed to understand these variations, but the performance is suitable for the application of interest here (meat spoilage detection, described below).

3.2 Characterization of the putrescine biosensor

The safety and quality control of food, particularly meats, are usually monitored through the detection of biogenic amines.[48] Previous putrescine biosensors have two major drawbacks: the relatively limited dynamic range[83] and slow response to exogenous toxic concentrations of

putrescine,[83, 89] which are not suitable to detect our target concentrations of putrescine in meats. Our goal is to be able to design a biosensor that would reflect the expected target concentrations of putrescine in its environment and achieve faster responses.[36, 82] We quantified the dose-response parameters for our synthetic promoters: (1) dynamic range which is the fold change in eGFP expression in the presence and absence of the analyte putrescine within the sample, (2) limit of detection (LOD) which is the lowest concentration of putrescine in a sample the biosensor is capable of detecting, and (3) sensitivity which describes the biosensor's ability to distinguish differences in putrescine concentration and the change in signal output when the putrescine concentration transitions from 0 mM to 1000 mM.

Dynamic range

Dynamic range is quantified as the ratio of the highest measured output to the lowest measured output.[101] A high dynamic range indicates an increased degree of confidence in the biosensors ability to measure a wide range of analyte concentrations.[102, 103] As shown in **Figure 2A**, we evaluated 6 synthetic promoters (3 controls) and the dynamic range values are generally higher for the synthetic promoters that we designed compared to the Chen *et al.* promoters; PuuAp, TacR(2), and LR2. For example, P_{hyb}(3A), showed a dynamic range of 186 ± 6.52 ($p < 0.0001$, $N = 3$ replicates), which is a ~30-fold increase compared to the dynamic range for PuuAp (5.54 ± 0.83). We also note the dynamic range for promoters with uniform binding sites are highest. For example, P_{hyb}(1B), which contains a B binding site between -35 and -10 and two A binding sites downstream of the -10, shows a similar dynamic range as the control promoters of 3.36 ± 3.74. Comparing with P_{hyb}(3B), which only contains B binding sites (at the same locations), shows a dramatic 17-fold increase in dynamic range. In fact, P_{hyb}(3A), P_{hyb}(3B), P_{hyb}(3C), all promoters

with uniform binding sites (at the same locations) all show similar dynamic range, ~ 178.3 ± 6.5, 156.1± 17.05, and 115.8 ± 25.05 respectively, and were observed to be the highest dynamic range of all synthetic promoters (with P_{hyb}(2C) as an exception).

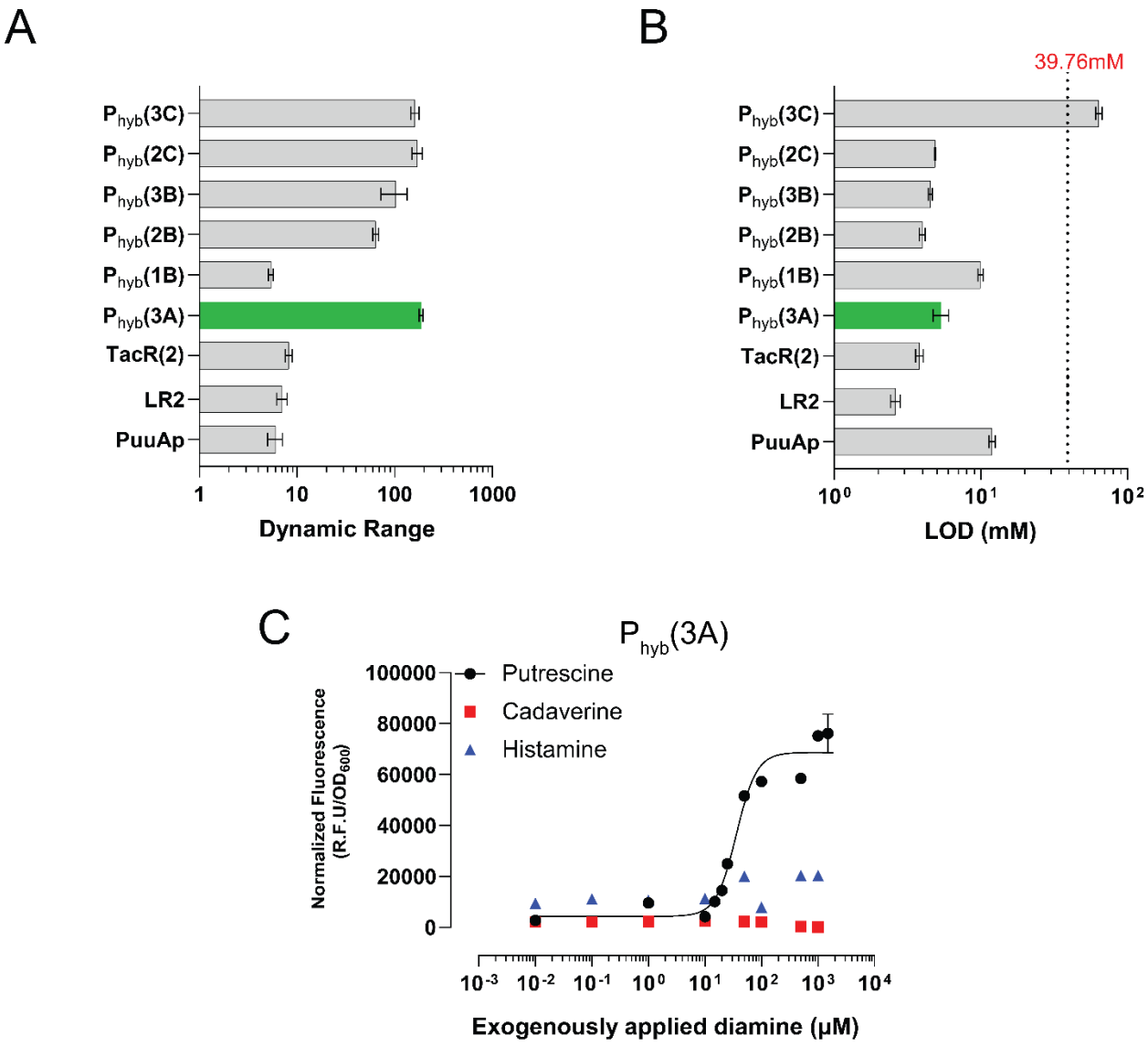

Figure 3.2 – Quantification of dose-response parameters for PuuR response promoters. (A) Dynamic range shown for Chen *et al.*[83] promoters: PuuAp, LR2, TacR(3), and TacR(2) and six hybrid promoters developed in this study. The promoter with the highest dynamic range, P_{hyb}(3A), is highlighted in green. (B) Limit of detection (LOD) shown for all 9 PuuR responsive promoters. The dotted line exhibits the target putrescine concentration (~ 39.76 mM). P_{hyb}(3A) has an LOD of 5.37 mM ± 0.66 and is highlighted in green. (C) Dose-response semi-log curve displays the normalized fluorescence (over OD) for different concentrations of putrescine, cadaverine, and histamine for promoter P_{hyb}(3A). All plots with error bars represent one standard error of mean (n = three independent replicates).

Limit of detection (LOD)

Currently, there is no well-defined legal putrescine limit in North America despite the ability of putrescine to accumulate in very high concentrations for many food products.[104, 105] However, one extensive study investigated the cytotoxic effects of putrescine when exposed to HT29 intestinal cells over a 24-hour period. The results showed that growth of HT29 cells were inhibited when putrescine reached a value of 39.8 mM or the half-maximal inhibitory concentration (IC_{50}).[53] We used this value as the defined limit of putrescine, and as shown in **Figure 2B,** we found all promoters (except for P_{hyb}(3C) to have an LOD lower than the target concentrations of putrescine. The LOD value was extrapolated from dose-response curves (**Figure S4)** and was found to be 5.37 mM ± 0.66, which is below the target 39.76 mM concentration.

Specificity

When constructing a biosensor for putrescine, there is a requirement to ensure strong and selective affinity between PuuR and the target analyte putrescine. Given that there are other biogenic amines that are similar to putrescine in chemical structure, we wanted to assess the crosstalk between different metabolites. We selected two chemically similar and naturally occurring biogenic amines: cadaverine (1,5-diaminopentane) and histamine (2,4-imidazolyl-ethylamine). Promoter P_{hyb}(3A) was treated with putrescine and two other biogenic amines cadaverine and histamine. As shown in **Figure 2C** (for completion, see **Figure S5** for other promoters), the dose-response curve showed minimal induction, where there is non-specific binding between PuuR and cadaverine and histamine resulting in a dynamic range close to zero. Significant lower percentages for histamine 2.5% ± 2.06 and cadaverine 2.84% ± 0.22 are observed for P_{hyb}(3A). These results are further supported by Chen *et al*., [83] who shows that PuuR is evolved to be highly specific to putrescine

and not towards other structurally similar biogenic amines (e.g., cadaverine). Given that P_{hyb}(3A) showed the optimal LOD, highest dynamic range, and minimal non-specific binding, we determined this promoter to be best suited for our meat sample sensor.

3.3 Cell-Free Biosensing

Cell-based biosensors are suitable for therapeutic applications[106] but are not suitable for spoiled meat detection given the culture conditions and equipment that are needed to maintain viability of the cells. To address this, we prepared our biosensor in a cell free system.[107-110] One of the key limitations with cell-free systems is that they are costly. Many of these studies use PURE-based (or commercial) cell-free systems because of strict quality control, however, it comes at a cost of ~ $ 3,383.00 USD, which translates to only 100 cell-free reactions.[111] To minimize cost, we constructed an in-house crude cell free system using Kwon *et al.* as a reference[87, 112], and from our calculations, we were able to minimize the cost from $33.83 USD per reaction to $1.52 USD/reaction using our cell-free system **(Table S7, Figure S6)**. Although creating an in-house cell free formulation can have significant cost benefits, there is the additional challenge of optimizing the system's parameters to enhance protein synthesis. To optimize our formulation for protein production, we tested two main parameters that affect cell-free protein synthesis: ion concentrations **(Figure S7A)** and lysate compositions **(Figure S7B)** since these parameters are known to have the largest effect in protein production.[87, 113, 114] Magnesium is an essential cofactor for DNA replication[115], transcription[116], and neutralizing the charge on ribosomal RNA (rRNA)[117]. Additionally, potassium ion concentrations need to be calibrated to stabilize functional mRNA, tRNA, and rRNA molecules.[118] From **Figure S7A**, we determined the optimal concentration for our cell-extract batch was 2 mM of magnesium and 20 mM of potassium for 30 μL lysate. We also examined the proportion of lysate composition necessary for our biosensor to properly

function and hypothesized that more lysate would result in higher eGFP transcription. However, the results indicated that with the energy, amino acids, and ions added to the solution, only 30 µL of cell-extract is required **(Figure S7B**) and this finding was corroborated by other cell-free biosensors.[35, 39, 119] In addition, we compared the protein production between our cell-free formulation and a commercial kit (Expressway™ Mini Cell-Free Expression System, Invitrogen) **(Figure 3A)**. Our formulation was shown to synthesize a higher protein yield in comparison to the commercial kit using our calibration curve. We produced 10.94 µg/mL ± 0.01 of eGFP protein in comparison to the commercial kit (Expressway™ Mini Cell-Free Expression System, Invitrogen) which produced 4.56 µg/mL ± 0.411 (a ~2.4-fold increase in eGFP yield). Next, we tested our cell-free system by supplementing the cell free reaction with a plasmid expressing eGFP under the control of a T7 promoter, and our formulation was able to express eGFP over a span of 8 hours (**Figure 3B)** which is suitable for our application below.

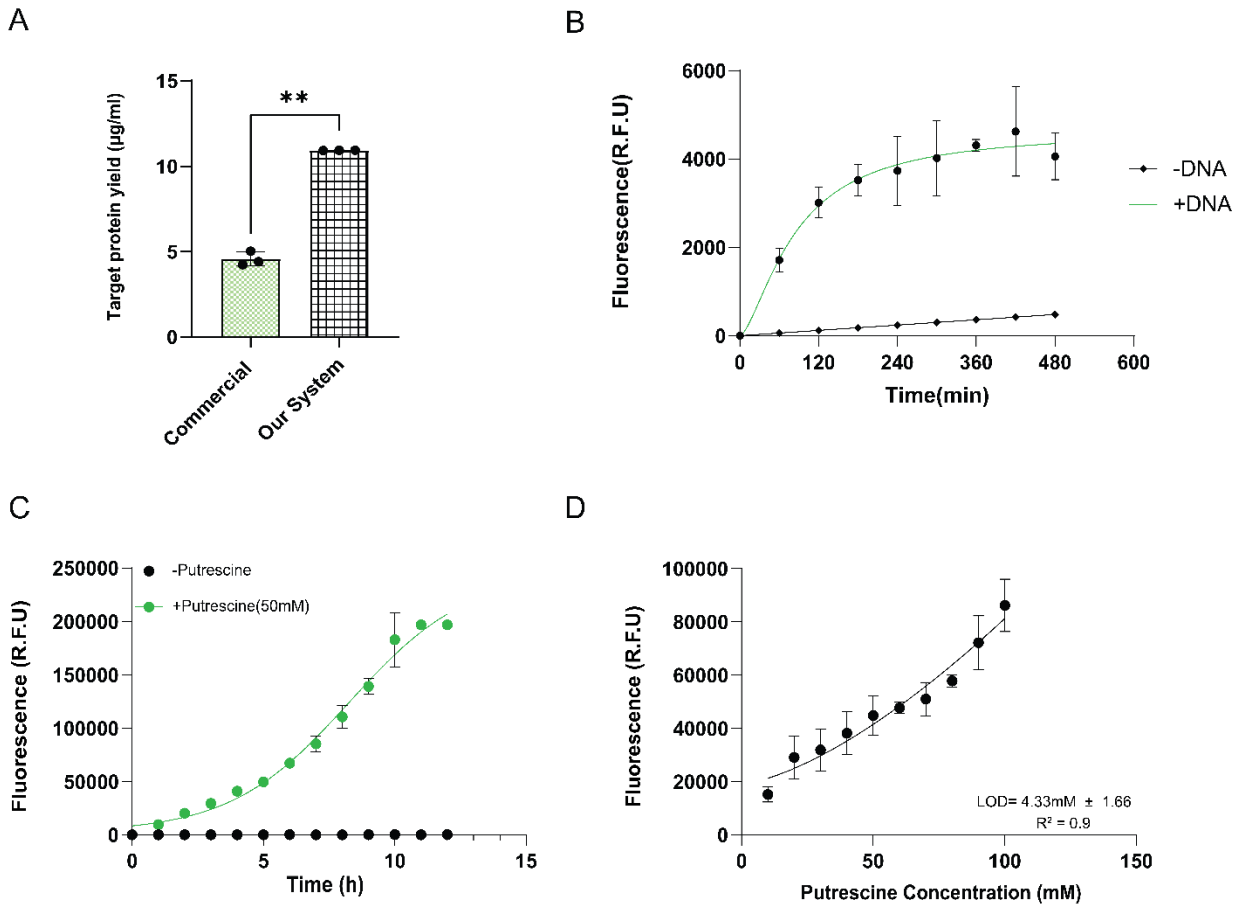

Figure 3.3 – Optimization of our in-house cell-free system. (A) Comparison of the total protein yield for our optimized cell-free reaction and a commercial lysate kit. Raw fluorescence values were converted to eGFP yield based on eGFP standard curve (see Figure S11). (B) Verification of in-home cell-free system, fluorescence over time in a cell-free biosensor system in a well-plate reader. (C) Spiked putrescine (50 mM) sample was added to cell-free biosensor on paper and measured over time in a well plate reader. Absence of putrescine in a cell-free reaction was performed as a control. (D) A calibration curve for P_{hyb}(3A) was generated to quantify fluorescent outputs (from our cell-free lysate) to putrescine concentration. Putrescine was exogenously added with a concentration range of 10 mM to 100 mM to the cell free reaction and incubated for 4 hours at 30 °C. All data point represents one standard deviation for two biological replicates.

3.4 Testing the biosensor with real meat samples

To evaluate the potential use of our cell-free biosensor in a field setting, we designed a paper-disc device that can be used to store our cell-free components and be used as a diagnostic device to determine the putrescine content in meats. We were motivated by previous works that have used freeze-dried paper discs for disease-based diagnostics [5, 120, 121] and designed four discs on one

device **(Figure S9)** and use the steps described by Mahmud *et al.*[88] to fabricate the paper-based discs. Following the workflow in **Figure S10**, cell free reactions were added to the paper discs, lyophilized for 12 hours, and putrescine standards or meat solution samples were added to the discs. As an initial test, we validated our cell-free biosensor system on paper by adding putrescine (50 mM) to the cell lysate and evaluating eGFP expression under the control of P_{hyb}(3A) over the course of 12 h. After 1 h, we already observe differences in the fluorescence (compared to the control), as shown in **Figure 3C.** Next, to evaluate the performance of the cell-free biosensor, a series of putrescine calibrators ranging from 10 – 100 mM was prepared and evaluated in triplicates. As shown in **Figure 3D**, the fluorescence response for the optimized promoter, P_{hyb}(3A), is fitted to the Hill equation, $R^2 = 0.9$, revealing a limit of detection of 4.33 mM ± 1.66 of putrescine, which is well below the defined limit for meat detection.

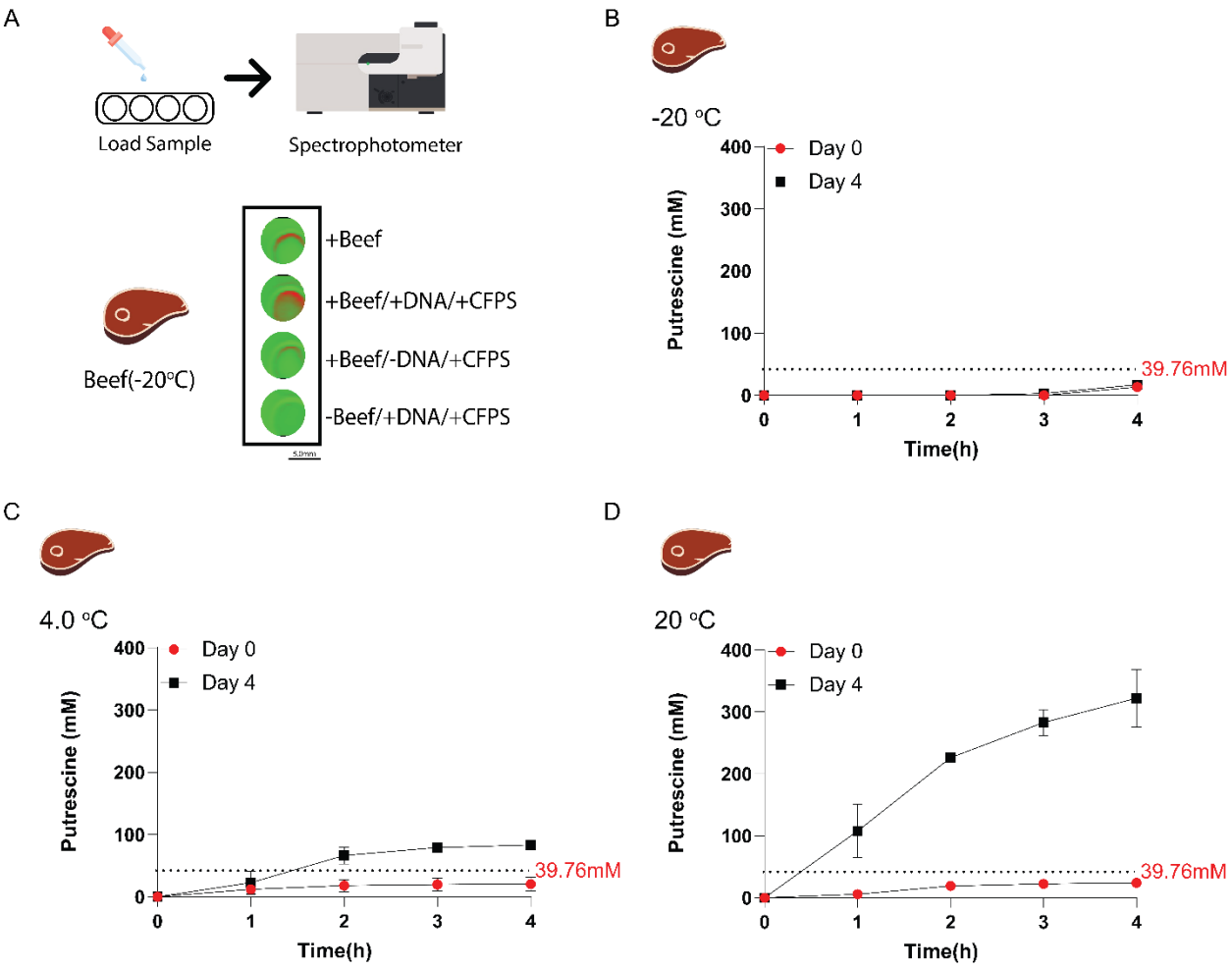

Figure 3.4 – Assessment of putrescine in beef using our FRSH device.(A) An image of the fluorescent well-scan after beef samples were stored at – 20 °C for four days. Each set of experiments contained four samples: only beef sample (+ beef), beef sample with cell-free biosensor (+beef/+DNA/+CFPS), beef sample and cell-free system (+beef/-DNA/+CFPS) and cell-free biosensor without beef sample (-beef/+DNA/+CFPS). (B-D) Kinetic plots showing the fluorescence of the putrescine content over 4 hours when stored under three temperatures (B) -20 °C, (C) 4 °C, and (D) 20 °C. Putrescine content was measured each hour on the paper discs. The error bars represent one standard deviation for three biological independent replicates.

Prepared beef samples were stored at different temperatures and their extractant was loaded onto paper devices, and spectrophotometer measurements were taken after four hours to measure putrescine content **(Figure 4A)**. **Figure 4(B-D)** presents our cell-free measurements of the kinetics for sensing putrescine in beef samples under different storage conditions. Each data point

represents the putrescine concentration (converted using calibration curve), $N = 3$, between 1 to 4 hours on either day 0 and 4 of storing the beef under fridge, room, or freezer temperature which are common forms of storage. As depicted, the temperature trend shows that freezer temperatures produce the lowest putrescine content and that room temperature show putrescine concentrations greater than the target concentration after 4 days. Although there was a foul smell for the beef after 1 day in room temperature, it is considered safe to eat when it is stored less than a day or when it is stored in the fridge and freezer for less than 4 days. This an expected result given the low temperature discourages bacterial populations from propagating and taking up free amines which can lead to enzymatic reactions to produce more putrescine.[64, 77]

As depicted in **Figure 4(B-D)**, the measurement was carried out after 4 hours of incubation. Measurable putrescine values were obtained for beef after 1 hour, especially at room temperature; however, saturation of these values were generally observed after 3 hours of incubation. This a notable result because our promoters show faster response times (compared to Chen *et al.*[83] promoters) when exposed to exogenous putrescine that is produced by real samples. We attribute the faster response times to having a cell-free system and an optimal promoter sequence for putrescine detection. Clearly, more work is required to improve the time to minutes, and we propose the time might be lowered by using different lysate or cell media formulations[83], RNA-based sensor[122], and non-fluorescence-based measurements[123]. However, the accuracy in determining the key trend and the target putrescine concentration gives us confidence that we are able to use our hybrid-based promoter with a cell-free system on paper discs to detect putrescine in real meat samples.

Chapter 4: Conclusion

Here I present our concluding remarks and future perspectives.

4.1 Conclusion

In summary, we have successfully used a cell-free paper biosensor for the detection of putrescine in different meat samples under different storage conditions. Using a systematic engineering approach, we improved biosensor performance by introducing TF-binding regions into promoters to make P_{hyb}(3A). This is an effective method to modulate dynamic range, sensitivity, background noise, LOD, and response time. A 3-fold increase in dynamic range was observed as a result of our promoter modifications. The biosensor showed a detection limit of 10.4 mM, which is lower than the toxic concentration of 39.76 mM, which induces cell necrosis in the intestinal lining. We further improved the system by incorporating cell-free biosensing with paper-sensing device making the device easy to use, portable, affordable, and biodegradable. We successfully demonstrated putrescine detection in real meat samples using the paper-based, cell-free paper biosensor. Taken together, this work could be expanded with additional TFs to include other BAs of relevance to the food industry such as spermidine, agmatine, and tyramine.

4.2 Future Perspectives

As we have highlighted, chemical procedures and instrumental methods used to monitor the quality of protein rich foods such as salmon, chicken, and beef are inconvenient for commercial use. Current methods have many limitations which make them impractical such as high cost, time-consuming, requires pretreatment of food samples, and a lot of the time requires skilled individuals to carry out the qualitative assay. Another trend adopted by many inspection agencies, like the FDA and CFIA, is the use of sensory evaluations using a trained panelist. Despite being a well-

established method to determine the quality of food freshness based on human sensors it can be time consuming subjective, our senses are less sensitive with time and when an individual is sick.[124] Assessing food quality is complex due to the intricate molecular nature of food, however we can reduce its complex nature by focusing on biomarkers that are indication of spoilage or increased microbial activity. One of the first BAs to be released during the process of spoilage happens to be putrescine and is at best the earliest indication hygienic contamination.

Previously published biosensors to detect putrescine lacked practicality in Chen *et al.* they built a tunable putrescine WCB using TFs for industrial purposes: monitoring endogenous putrescine biosynthesis. In Zhang *et al.* they developed a WCB using TFs for diamine biosensor, however it lacked specificity towards putrescine. Our cell-free putrescine TF based biosensor eliminates the time and specialized equipment associated with culturing cells to determine the putrescine content in food samples. Our successful development of an easy-to-use putrescine specific cell-free paper biosensor has the potential to extend its reach to individuals from diverse backgrounds; from the sous-chef checking the quality of an expensive wagyu beef, to the butcher or fishmonger checking their stock of meats, to the everyday parent unsure of the freshness of the meat. However, a lot more work is required before FRSH-test becomes as a ubiquitous as a pregnancy test. To improve the FRSH test we suggest the following integrating a high-quality CFPS system to decrease response time from 4 hours to preferably 30 min. Secondly the use of a colorimetric signal instead of a fluorescent signal eliminates the need for a spectrophotometer and can easily be read with the naked eye. Thirdly, a digital read much like glucose sensor to facilitate comprehension of assay results which avoids confusion.

The abundance of protein-rich foods like cheese and wine opens the possibilities of testing quality and flavor profiles that maybe affected by putrescine contamination with our biosensor.

Taken together, our engineering cell-free putrescine biosensor decentralizes sensing technology and has the potential to empower consumers to monitor and ensure quality control within their own home.

References

[1] Huggett, A. S., and Nixon, D. A. (1957) Use of glucose oxidase, peroxidase, and O-dianisidine in determination of blood and urinary glucose, *Lancet*, 368-370.

[2] Ragavan, K. V., and Neethiraja, S. (2019) *Chapter 7 - Nanoparticles as Biosensors for Food Quality and Safety Assessment*, Elsevier.

[3] Thakur, M. S., and Ragavan, K. V. (2013) Biosensors in food processing, *J Food Sci Technol 50*, 625-641.

[4] Mehrotra, P. (2016) Biosensors and their applications - A review, *J Oral Biol Craniofac Res 6*, 153-159.

[5] Thavarajah, W., Silverman, A. D., Verosloff, M. S., Kelley-Loughnane, N., Jewett, M. C., and Lucks, J. B. (2020) Point-of-Use Detection of Environmental Fluoride via a Cell-Free Riboswitch-Based Biosensor, *ACS Synth Biol 9*, 10-18.

[6] Bhalla, N., Jolly, P., Formisano, N., and Estrela, P. (2016) Introduction to biosensors, *Essays Biochem 60*, 1-8.

[7] Constantin, N. T. (2021) Can Wheat Germination Test Be Used to Predict Pregnancy in Ewes?, *Bulletin of University of Agricultural Sciences and Veterinary Medicine Cluj-Napoca: Veterinary Medicine 78*, 29-37.

[8] Rayford, P. L., Vaitukaitis, J. L., Ross, G. T., Morgan, F. J., and Canfield, R. E. (1972) Use of specific antisera to characterize biologic activity of hCG-beta subunit preparations, *Endocrinology 91*, 144–146.

[9] Vaitukaitis, J. L., Braunstein, G. D., and Ross, G. T. (1972) A radioimmunoassay which specifically measures human chorionic gonadotropin in the presence of human luteinizing hormone, *American Journal of Obstetrics and Gynecology 6*, 751–758.

[10] Gamba, J. M. (2012) The role of transport phenomena in whispering gallery mode optical biosensor performance, In *Chemical Engineering*, California Institute of Technology, Pasadena, California, USA.

[11] Veeradasan, P., and Uda H. (2014) Advances in biosensors: Principle, architecture and applications, *Journal of Applied Biomedicine 12*, 1-15.

[12] Jameson, K. R., Christopher, D. G., Noah, D. T., Srivatsan, R., Kelley, A., and George, M. C. (2015) Synthetic biosensors for precise gene control and real-time monitoring of metabolites, *Nucleic Acids Research 43*, 7648–7660.

[13] Ahmad, M. A., Di, L., Fuzhong, Z., and Diego, A. O. (2017) Fundamental Design Principles for Transcription-Factor-Based Metabolite Biosensors, *ACS Synthetic Biology 6*, 1851-1859.

[14] J. Castillo, S. Gáspár, S. Leth, M. Niculescu, A. Mortari, I. Bontidean, V. Soukharev, S.A. Dorneanu, A.D. Ryabov, and E. Csöregi. (2004) Biosensors for life quality: Design, development and applications, *Sensors and Actuators B: Chemical 102*, 179-194.

[15] Nguyen, H. H., Lee, S. H., Lee, U. J., Fermin, C. D., and Kim, M. (2019) Immobilized Enzymes in Biosensor Applications, *Materials (Basel) 12*, 1-34.

[16] Rocchitta, G., Spanu, A., Babudieri, S., Latte, G., Madeddu, G., Galleri, G., Nuvoli, S., Bagella, P., Demartis, M. I., Fiore, V., Manetti, R., and Serra, P. A. (2016) Enzyme Biosensors for Biomedical Applications: Strategies for Safeguarding Analytical Performances in Biological Fluids, *Sensors (Basel) 16*, 1-21.

[17] Yeom, S. J., Kim, M., Kwon, K. K., Fu, Y., Rha, E., Park, S. H., Lee, H., Kim, H., Lee, D. H., Kim, D. M., and Lee, S. G. (2018) A synthetic microbial biosensor for high-throughput screening of lactam biocatalysts, *Nat Commun 9*, 50-53.

[18] Sharma, S., Byrne, H., and O'Kennedy, R. J. (2016) Antibodies and antibody-derived analytical biosensors, *Essays Biochem 60*, 9-18.

[19] Castillo-Henriquez, L., Brenes-Acuna, M., Castro-Rojas, A., Cordero-Salmeron, R., Lopretti-Correa, M., and Vega-Baudrit, J. R. (2020) Biosensors for the Detection of Bacterial and Viral Clinical Pathogens, *Sensors (Basel) 20*, 1-19.
[20] Chen, S. Y., Wei, W., Yin, B. C., Tong, Y., Lu, J., and Ye, B. C. (2019) Development of a Highly Sensitive Whole-Cell Biosensor for Arsenite Detection through Engineered Promoter Modifications, *ACS Synth Biol 8*, 2295-2302.
[21] Torsten, S., Alina, E., Thomas, S., and Johanna, W. (2018) Aptamer-based lateral flow assays, *AIMS Bioengineering 5*, 78-102.
[22] Ye, W., Liu, T., Zhang, W., Zhu, M., Liu, Z., Kong, Y., and Liu, S. (2019) Marine Toxins Detection by Biosensors Based on Aptamers, *Toxins (Basel) 12*, 1-22.
[23] Yazdanparast, S., Benvidi, A., Banaei, M., Nikukar, H., Tezerjani, M. D., and Azimzadeh, M. (2018) Dual-aptamer based electrochemical sandwich biosensor for MCF-7 human breast cancer cells using silver nanoparticle labels and a poly(glutamic acid)/MWNT nanocomposite, *Mikrochim Acta 185*, 1-10.
[24] Zhang, F., Carothers, J. M., and Keasling, J. D. (2012) Design of a dynamic sensor-regulator system for production of chemicals and fuels derived from fatty acids, *Nat Biotechnol 30*, 354-359.
[25] Jaspreet, K., Sandeep, C., Rashmi, C., Rahul, D. J., and Abhijeet, J. (2019) Enzyme-based biosensors, *Bioelectronics and Medical Devices*, 211-240.
[26] Atkinson, A. L., and Haggett, B. G. D. (1993) Whole Cell Biosensors for Environmental Monitoring, *Sensor Review 13*, 19-22.
[27] Gui, Q., Lawson, T., Shan, S., Yan, L., and Liu, Y. (2017) The Application of Whole Cell-Based Biosensors for Use in Environmental Analysis and in Medical Diagnostics, *Sensors (Basel) 17*, 1-17.
[28] Koch, M., Pandi, A., Borkowski, O., Batista, A. C., and Faulon, J. L. (2019) Custom-made transcriptional biosensors for metabolic engineering, *Curr Opin Biotechnol 59*, 78-84.
[29] McConnell, E. M., Nguyen, J., and Li, Y. (2020) Aptamer-Based Biosensors for Environmental Monitoring *Frontiers in Chemistry 8* 1-24.
[30] Chai, C., Xie, Z., and Grotewold, E. (2011) SELEX (Systematic Evolution of Ligands by EXponential Enrichment), as a powerful tool for deciphering the protein-DNA interaction space, *Methods Mol Biol 754*, 249-258.
[31] Cheng, F., Tang, X. L., and Kardashliev, T. (2018) Transcription Factor-Based Biosensors in High-Throughput Screening: Advances and Applications, *Biotechnol J 13*, e1700648.
[32] Schallmey, M., Frunzke, J., Eggeling, L., and Marienhagen, J. (2014) Looking for the pick of the bunch: high-throughput screening of producing microorganisms with biosensors, *Curr Opin Biotechnol 26*, 148-154.
[33] Beckwith, J. R. (1967) Regulation of the lac operon. Recent studies on the regulation of lactose metabolism in Escherichia coli support the operon model, *Science 156*, 597-604.
[34] Raul, F. L., Raul, R., Fernando, D. C., and Gabriel, M. (2015) Transcription factor-based biosensors enlightened by the analyte, *Frontiers in Microbiology 6*, 1-21.
[35] Voyvodic, P. L., Pandi, A., Koch, M., Conejero, I., Valjent, E., Courtet, P., Renard, E., Faulon, J. L., and Bonnet, J. (2019) Plug-and-play metabolic transducers expand the chemical detection space of cell-free biosensors, *Nat Commun 10*, 1-8.
[36] Ding, N., Zhou, S., and Deng, Y. (2021) Transcription-Factor-based Biosensor Engineering for Applications in Synthetic Biology, *ACS Synth Biol 10*, 911-922.
[37] Young, B. P., Shin, J. J., Orij, R., Chao, J. T., Li, S. C., Guan, X. L., Khong, A., Jan, E., Wenk, M. R., Prinz, W. A., Smits, G. J., and Loewen, C. J. (2010) Phosphatidic acid is a pH biosensor that links membrane biogenesis to metabolism, *Science 329*, 1085-1088.
[38] Mahr, R., and Frunzke, J. (2016) Transcription factor-based biosensors in biotechnology: current state and future prospects, *Appl Microbiol Biotechnol 100*, 79-90.
[39] Jung, J. K., Alam, K. K., Verosloff, M. S., Capdevila, D. A., Desmau, M., Clauer, P. R., Lee, J. W., Nguyen, P. Q., Pasten, P. A., Matiasek, S. J., Gaillard, J. F., Giedroc, D. P., Collins, J. J., and

Lucks, J. B. (2020) Cell-free biosensors for rapid detection of water contaminants, *Nat Biotechnol 38*, 1451-1459.
[40] Khambhati, K., Bhattacharjee, G., Gohil, N., Braddick, D., Kulkarni, V., and Singh, V. (2019) Exploring the Potential of Cell-Free Protein Synthesis for Extending the Abilities of Biological Systems, *Front Bioeng Biotechnol 7*, 1-16.
[41] Lee, K. H., and Kim, D. M. (2019) In Vitro Use of Cellular Synthetic Machinery for Biosensing Applications, *Front Pharmacol 10*, 1166.
[42] Hodgman, C. E., and Jewett, M. C. (2012) Cell-free synthetic biology: thinking outside the cell, *Metab Eng 14*, 261-269.
[43] Swartz, J. R. (2012) Transforming biochemical engineering with cell-free biology, *AIChE Journal 58*, 5–13.
[44] Hodgman, C. E., and Jewett, M. C. (2013) Optimized extract preparation methods and reaction conditions for improved yeast cell-free protein synthesis, *Biotechnol Bioeng 110*, 2643-2654.
[45] Perez, J. G., Stark, J. C., and Jewett, M. C. (2016) Cell-Free Synthetic Biology: Engineering Beyond the Cell, *Cold Spring Harb Perspect Biol 8*, a023853.
[46] Zhang, L., Guo, W., and Lu, Y. (2020) Advances in Cell-Free Biosensors: Principle, Mechanism, and Applications, *Biotechnol J 15*, e2000187.
[47] Ahmad, M. A., Di, L., Fuzhong, Z., and Diego, A. O. (2017) Fundamental Design Principles for Transcription-Factor-Based Metabolite Biosensors, *ACS Synth Biol 6*, 1851-1859.
[48] John, D. C., Birgit, N., Herbert, B., Olivier, A., Sava, B., John, G., Tine, H., Arie, H., James, H., Günter, K., Kostas, K., James, M., Christine, M., Christophe, N., and Luisa, P. (2011) Scientific Opinion on risk based control of biogenic amine formation in fermented foods, *European Food Safety Authority (EFSA) 9*, 1-93.
[49] Xiulai, C., Cong, G., Liang, G., Guipeng, H., Qiuling, L., Jia, L., Jens, N., Jian, C., and Liming, L. (2018) DCEO Biotechnology: Tools To Design, Construct, Evaluate, and Optimize the Metabolic Pathway for Biosynthesis of Chemicals, *ACS Synbio: Chemical Review 118*, 4-72.
[50] Ashiq, H., Luis, R. S., David, M. F., Gaurav, A., Venkatesh, S. K., Stephen, D. L., and Sigrun, I. K. (2013) "High-affinity olfactory receptor for the death-associated odor cadaverine.", *Proceedings of the National Academy of Sciences 110*, 19579-19584.
[51] Cristina I., José, C. G. T., Jean-Christophe, N., Leonardo, P., and Angel, G. (2018) Identifying human diamine sensors for death related putrescine and cadaverine molecules, *PLoS Computational Biology 14*, e1005945.
[52] Jessica, D., Christine, F., Georges, L., Yves, B., Francois, J. V., and Eric, H. (2013) Electrophysiological and Behavioral Responses of Thanatophilus sinuatus Fabricius (Coleoptera: Silphidae) to Selected Cadaveric Volatile Organic Compounds, *Journal of Forensics Science 58*, 917-923.
[53] Beatriz del Rio, Begoña Redruello, Daniel M. Linares, Victor Ladero, Patricia Ruas-Madiedo, Maria Fernandez, M. Cruz M., and A.A., M. (2019) The biogenic amines putrescine and cadaverine show in vitro cytotoxicity at concentrations that can be found in foods, *120*, 1-7.
[54] Ruiz-Capillas, C., and Herrero, A. M. (2019) Impact of Biogenic Amines on Food Quality and Safety, *Foods 8*, 1-16.
[55] Naila, A., Flint, S., Fletcher, G., Bremer, P., and Meerdink, G. (2010) Control of biogenic amines in food--existing and emerging approaches, *J Food Sci 75*, 139-150.
[56] Benito, S. (2019) The management of compounds that influence human health in modern winemaking from an HACCP point of view, *Fermentation 5*, 1-20.
[57] Kleter, G. A., and Marvin, H. J. (2009) Indicators of emerging hazards and risks to food safety, *.Food Chem Toxicology*, 1022-1039.
[58] AFFAIRS, F. A. D. A. O. O. R. (2020) Sensory Analysis ((FDA), F. A. D. A. O., Ed.).
[59] Doeun, D., Davaatseren, M., and Chung, M. S. (2017) Biogenic amines in foods, *Food Sci Biotechnol 26*, 1463-1474.

[60] Pekka, L. (1996) Determination of amines and amino acids in wine, a review, *Am J Enol Vitic 47*, 127–133.
[61] Gardini, F., Ozogul, Y., Suzzi, G., Tabanelli, G., and Ozogul, F. (2016) Technological Factors Affecting Biogenic Amine Content in Foods: A Review, *Front Microbiol 7*, 1-18.
[62] Russo, P., Giuseppe, S., Vittorio, C., Daniela, F., Francesco, G., and Luciano, B. (2010) Are consumers aware of the risks related to Biogenic Amines in food., *Curr Res. Technol. Edu. Top. Appl. Microbiol. Microb. Biotechnol*, 1087-1095.
[63] Atiya Ali, M., Poortvliet, E., Stromberg, R., and Yngve, A. (2011) Polyamines in foods: development of a food database, *Food Nutr Res 55*, 1-16.
[64] Vinci, G., and Antonelli, M. L. (2002) Biogenic amines: quality index of freshness in red and white meat, *Food Control 13*, 519-524.
[65] Triki, M., Herrero, A. M., Jimenez-Colmenero, F., and Ruiz-Capillas, C. (2018) Quality Assessment of Fresh Meat from Several Species Based on Free Amino Acid and Biogenic Amine Contents during Chilled Storage, *Foods 7*, 1-16.
[66] Karmas, E. (1981) Biogenic amines as indicators of seafood freshness. , *Food Sci. Technol. 17*, 20-23.
[67] Hernandez-Jover, T., Izquierdo-Pulido, M., Veciana-Nogues, M. T., and Vidal-Carou, M. C. (1996) Ion-pair high-performance liquid chromatographic determination of biogenic amines in meat and meat products, *J Agric Food Chem. 44*, 2710–2715.
[68] Leona, W., Leona, B., Marek, K., Petra, J., and Frantisek, B. (2014) Formation, Degradation, and Detoxification of Putrescine by Foodborne Bacteria: A Review, *Comprehensive Reviewsin Food Science and Food Safety 13*, 1012-1030.
[69] Soda, K., Kano, Y., Sakuragi, M., Takao, K., Lefor, A., and Konishi, F. (2009) Long-term oral polyamine intake increases blood polyamines concentrations, *J Nutr Sci Vitaminol 55*, 361–366.
[70] Zdrojewicz, Z., and Lachowski, M. (2014) The importance of putrescine in the human body, *Europe PMC 68*, 393-403.
[71] Ramani, D., De Bandt, J. P., and Cynober, L. (2014) Aliphatic polyamines in physiology and diseases, *Clinical Nutrition 33*, 14-22.
[72] Giuseppe, L., Gianluca, P., and Luciano, D. A. (2012) DNA and nuclear aggregates of polyamines, *Biochimica et Biophysica Acta (BBA) - Molecular Cell Research 1823*, 1745-1755.
[73] Medina, M. A., Urdiales, J. L., Rodriguez-Caso, C., Ram´ırez, F. J., and Sanchez, J. (2003) Biogenic amines and polyamines: similar biochemistry for different physiological missions and biomedical applications, *Crit Rev Biochem Mol biol 38*, 23-59.
[74] Santos, S. (1996) Biogenic amines: their importance in foods., *Intl Journal Food Microbiology 29*, 213-231.
[75] Pegg, A. E. (2009) Mammalian polyamine metabolism and function. IUBMB Life, *IUBMB Life 61*, 880-894.
[76] Plenis, A., Oledzka, I., Kowalski, P., Miekus, N., and Baczek, T. (2019) Recent Trends in the Quantification of Biogenic Amines in Biofluids as Biomarkers of Various Disorders: A Review, *Journal of clinical medicine 8*, 1-55.
[77] Wunderlichová, L., Buňková, L., Koutný, M., Jančová, P., and Buňka, F. (2014) Formation, degradation, and detoxification of putrescine by foodborne bacteria: A review *Comprehensive Review Food Science and Food Safety 13*, 1012–1030.
[78] Green, M. R., and Sambrook, J. (2018) The Hanahan Method for Preparation and Transformation of Competent Escherichia coli : High-Efficiency Transformation. Cold Spring Harbor Protocols, 2018(3), pdb.prot101188. d, *Cold Spring Harbor Protocols 3*, 183-190.
[79] Linshiz, G., Stawski, N., Goyal, G., Bi, C., Poust, S., Sharma, M., Mutalik, V., Keasling, J. D., and Hillson, N. J. (2014) PR-PR: cross-platform laboratory automation system., *ACS Synth Biol. 15*, 515-524.

[80] Moore, S. J., Lai, H. E., Kelwick, R. J., Chee, S. M., Bell, D. J., Polizzi, K. M., and Freemont, P. S. (2016) EcoFlex: A Multifunctional MoClo Kit for E. coli Synthetic Biology, *ACS Synth Biol 5*, 1059-1069.
[81] Perry, J. M., Soffer, G., Jain, R., and Shih, S. C. C. (2021) Expanding the limits towards 'one-pot' DNA assembly and transformation on a rapid-prototype microfluidic device, *Lab Chip 21*, 3730-3741.
[82] Chen, X., Gao, C., Guo, L., Hu, G., Luo, Q., Liu, J., and Liu, L. (2017) DCEO Biotechnology: Tools To Design, Construct, Evaluate, and Optimize the Metabolic Pathway for Biosynthesis of Chemicals, *ACS Synth Biol 118*, 26-27.
[83] Chen, X. F., Xia, X. X., Lee, S. Y., and Qian, Z. G. (2018) Engineering tunable biosensors for monitoring putrescine in Escherichia coli, *Biotechnol Bioeng 115*, 1014-1027.
[84] De Paepe, B., Peters, G., Coussement, P., Maertens, J., and De Mey, M. (2017) Tailor-made transcriptional biosensors for optimizing microbial cell factories, *J Ind Microbiol Biotechnol 44*, 623-645.
[85] Thompson, M. G., Costello, Z., Hummel, N. F. C., Cruz-Morales, P., Blake-Hedges, J. M., Krishna, R. N., Skyrud, W., Pearson, A. N., Incha, M. R., Shih, P. M., Garcia-Martin, H., and Keasling, J. D. (2019) Robust Characterization of Two Distinct Glutarate Sensing Transcription Factors of Pseudomonas putida l-Lysine Metabolism, *ACS Synth Biol 8*, 2385-2396.
[86] Armbruster, D. A., and Pry, T. (2008) Limit of blank, limit of detection and limit of quantitation, *Clin Biochem Rev 29 Suppl 1*, 49-52.
[87] Levine, M. Z., Gregorio, N. E., Jewett, M. C., Watts, K. R., and Oza, J. P. (2019) Escherichia coli-Based Cell-Free Protein Synthesis: Protocols for a robust, flexible, and accessible platform technology, *J Vis Exp*, e58882.
[88] Mahmud, M. A., Blondeel, E. J., Kaddoura, M., and MacDonald, B. D. (2016) Creating compact and microscale features in paper-based devices by laser cutting, *Analyst 141*, 6449-6454.
[89] Zhao, N., Song, J., Zhang, H., Lin, Y., Han, S., Huang, Y., and Zheng, S. (2021) Development of a Transcription Factor-Based Diamine Biosensor in Corynebacterium glutamicum, *ACS Synth Biol 10*, 3074-3083.
[90] Amann, E., Ochs, B., and Abel, K. J. (1988) Tightly regulated tac promoter vectors useful for the expression of unfused and fused proteins in Escherichia coli, *Gene 69*, 301-315.
[91] de Boer, H. A., Comstock, L. J., and Vasser, M. (1983) The tac promoter: a functional hybrid derived from the trp and lac promoters, *Proc Natl Acad Sci U S A 80*, 21-25.
[92] Knaus, R., and Bujard, H. (1988) PL of coliphage lambda: an alternative solution for an efficient promoter, *EMBO J 7*, 2919-2923.
[93] Park, Y., Kim, S. M., Lee, J. Y., and Jang, W. (2015) Application of biosensors in smart packaging, *Molecular & Cellular Toxicology*, 277-285.
[94] Teot, L., and Deschamps, F. (1990) [Histologic and echographic correlations of the hip in newborn infants], *Rev Chir Orthop Reparatrice Appar Mot 76*, 8-16.
[95] John, B., and Hal, S. A. (2012) Promoter engineering: Recent advances in controlling transcription at the most fundamental level, *Biotechnology journal 8*, 46-58.
[96] Nemoto, N., Kurihara, S., Kitahara, Y., Asada, K., Kato, K., and Suzuki, H. (2012) Mechanism for regulation of the putrescine utilization pathway by the transcription factor PuuR in Escherichia coli K-12, *J Bacteriol 194*, 3437-3447.
[97] Kurihara, S., Tsuboi, Y., Oda, S., Kim, H. G., Kumagai, H., and Suzuki, H. (2009) The putrescine Importer PuuP of Escherichia coli K-12, *J Bacteriol 191*, 2776-2782.
[98] Collado-Vides, J., Magasanik, B., and Gralla, J. D. (1991) Control site location and transcriptional regulation in Escherichia coli, *Microbiol Rev 55*, 371-394.
[99] Crocker, J., Noon, E. P., and Stern, D. L. (2016) The Soft Touch: Low-Affinity Transcription Factor Binding Sites in Development and Evolution, *Curr Top Dev Biol 117*, 455-469.
[100] David, A. A., and Terry, P. (2008) Limit of Blank, Limit of Detection and Limit of Quantitation, *The clinical biochemist review 29*, 49-52.

[101] Rogers, J. K., Taylor, N. D., and Church, G. M. (2016) Biosensor-based engineering of biosynthetic pathways, *Curr Opin Biotechnol 42*, 84-91.
[102] Berepiki, A., Kent, R., Machado, L. F. M., and Dixon, N. (2020) Development of High-Performance Whole Cell Biosensors Aided by Statistical Modeling, *ACS Synth Biol 9*, 576-589.
[103] Chou, H. H., and Keasling, J. D. (2013) Programming adaptive control to evolve increased metabolite production, *Nat Commun 4*, 1-8.
[104] Mohamed, A. A., Eric, P., Roger, S., and Agneta, Y. (2011) Polyamines in foods: development of a food database, *Food & Nutrition Research 55*, 1-15.
[105] Elke, R. G., Robert, G., Werner, B., Roland, G., Friedrich, B., and Peter, P. (2012) Dietary exposure assessment of putrescine and cadaverine and derivation of tolerable levels in selected foods consumed in Austria, *European Food and Technology 235*, 209–220.
[106] Bloemberg, D., Nguyen, T., MacLean, S., Zafer, A., Gadoury, C., Gurnani, K., Chattopadhyay, A., Ash, J., Lippens, J., Harcus, D., Page, M., Fortin, A., Pon, R. A., Gilbert, R., Marcil, A., Weeratna, R. D., and McComb, S. (2020) A High-Throughput Method for Characterizing Novel Chimeric Antigen Receptors in Jurkat Cells, *Mol Ther Methods Clin Dev 16*, 238-254.
[107] Sheng-Yan, C., Wenping, W., Bin-Cheng, Y., Yanbin, T., Jianjiang, L., and Bang-Ce, Y. (2019) Development of a Highly Sensitive Whole-Cell Biosensor for Arsenite Detection through Engineered Promoter Modifications, *ACS Synth. Biol. 8*, 2295−2302.
[108] Aidan, T., Yu, Z., Fan, H., Kirstie, L. S., Anli, A. T., Alexander, A. G., and P., K. (2020) *Cell-free biosensors: synthetic biology without borders. Handbook of Cell Biosensors*, Springer International Publishing, La Roche-sur-Yon, France.
[109] Zhang, L., Wei, G., and Yuan, L. (2020) Advances in Cell-Free Biosensors: Principle, Mechanism, and Applications, *Biotechnology Journal 15*, 1-16.
[110] Grawe, A., Dreyer, A., Vornholt, T., Barteczko, U., Buchholz, L., Drews, G., Ho, U. L., Jackowski, M. E., Kracht, M., Luders, J., Bleckwehl, T., Rositzka, L., Ruwe, M., Wittchen, M., Lutter, P., Muller, K., and Kalinowski, J. (2019) A paper-based, cell-free biosensor system for the detection of heavy metals and date rape drugs, *PLoS One 14*, e0210940.
[111] Barbora, L., and Sebastian, J. M. (2019) A simple, robust, and low-cost method to produce the PURE cell - free system., *ACS Synthetic Biology 8* 455-462.
[112] Kwon, Y. C., and Jewett, M. C. (2015) High-throughput preparation methods of crude extract for robust cell-free protein synthesis, *Sci Rep 5*, 1-8.
[113] Silverman, A. D., Kelley-Loughnane, N., Lucks, J. B., and Jewett, M. C. (2019) Deconstructing Cell-Free Extract Preparation for in Vitro Activation of Transcriptional Genetic Circuitry, *ACS Synth Biol 8*, 403-414.
[114] Yang, W. C., Patel, K. G., Wong, H. E., and Swartz, J. R. (2012) Simplifying and streamlining Escherichia coli-based cell-free protein synthesis, *Biotechnol Prog 28*, 413-420.
[115] Hartwig, A. (2001) Role of magnesium in genomic stability, *Mutation Research/Fundamental and Molecular Mechanisms of Mutagenesis 475*, 113-121.
[116] Misra, V. K., and Draper, D. E. (2002) The linkage between magnesium binding and RNA folding, *J Mol Biol 317*, 507-521.
[117] Pontes, M. H., Yeom, J., and Groisman, E. A. (2016) Reducing Ribosome Biosynthesis Promotes Translation during Low Mg(2+) Stress, *Mol Cell 64*, 480-492.
[118] Rozov, A., Khusainov, I., El Omari, K., Duman, R., Mykhaylyk, V., Yusupov, M., Westhof, E., Wagner, A., and Yusupova, G. (2019) Importance of potassium ions for ribosome structure and function revealed by long-wavelength X-ray diffraction, *Nat Commun 10*, 1-12.
[119] Pandi, A., Grigoras, I., Borkowski, O., and Faulon, J. L. (2019) Optimizing Cell-Free Biosensors to Monitor Enzymatic Production, *ACS Synth Biol 8*, 1952-1957.
[120] Pardee, K., Green, A. A., Ferrante, T., Cameron, D. E., DaleyKeyser, A., Yin, P., and Collins, J. J. (2014) Paper-based synthetic gene networks, *Cell 159*, 940-954.
[121] Didovyk, A., Tonooka, T., Tsimring, L., and Hasty, J. (2017) Rapid and Scalable Preparation of Bacterial Lysates for Cell-Free Gene Expression, *ACS Synth Biol 6*, 2198-2208.

[122] Karlikow, M., da Silva, S. J. R., Guo, Y., Cicek, S., Krokovsky, L., Homme, P., Xiong, Y., Xu, T., Calderon-Pelaez, M. A., Camacho-Ortega, S., Ma, D., de Magalhaes, J. J. F., Souza, B., de Albuquerque Cabral, D. G., Jaenes, K., Sutyrina, P., Ferrante, T., Benitez, A. D., Nipaz, V., Ponce, P., Rackus, D. G., Collins, J. J., Paiva, M., Castellanos, J. E., Cevallos, V., Green, A. A., Ayres, C., Pena, L., and Pardee, K. (2022) Field validation of the performance of paper-based tests for the detection of the Zika and chikungunya viruses in serum samples, *Nat Biomed Eng 6*, 246-256.

[123] Sadat Mousavi, P., Smith, S. J., Chen, J. B., Karlikow, M., Tinafar, A., Robinson, C., Liu, W., Ma, D., Green, A. A., Kelley, S. O., and Pardee, K. (2020) A multiplexed, electrochemical interface for gene-circuit-based sensors, *Nat Chem 12*, 48-55.

[124] Zaukuu, J. L. Z., Bazar, G., Gillay, Z., and Kovacs, Z. (2020) Emerging trends of advanced sensor based instruments for meat, poultry and fish quality– a review, *Critical Reviews in Food Science and Nutrition 60*, 3443-3460.

[125] Kurihara, S., Oda, S., Tsuboi, Y., Kim, H. G., Oshida, M., Kumagai, H., and Suzuki, H. (2008) gamma-Glutamylputrescine synthetase in the putrescine utilization pathway of Escherichia coli K-12, *J Biol Chem 283*, 19981-19990.

[126] Terui, Y., Saroj, S. D., Sakamoto, A., Yoshida, T., Higashi, K., Kurihara, S., Suzuki, H., Toida, T., Kashiwagi, K., and Igarashi, K. (2014) Properties of putrescine uptake by PotFGHI and PuuP and their physiological significance in Escherichia coli, *Amino Acids 46*, 661-670.

Supplementary Information

Protocol S1: Generating Golden Gate destination vector for repressor plasmid

BsaI restriction sites were inserted into the pFAB4876 backbone by performing two cycles of PCR. Primers were designed to incorporate the BsaI site into the 5´end of the forward primer while the reverse primer anneals back-to-back with the 5´end of the complementary region of the forward primer, refer to **Figure S2**. In the first cycle of PCR, the primer pair pFAB4876_frwd_BsaI and pFAB4876_rev_BsaI (Table 1) were used in a 50 µl PCR reaction containing 43.5µl G/C master mix, 2.5µl forward, 2.5µl reverse primer, 1.0µl of template, and 0.5µl Phusion® high-fidelity DNA polymerase (NEB) and was mixed by pipetting up and down. First round of PCR conditions are listed in **(Supplementary Table 5)**. Methylated template DNA was removed after PCR by restriction digest using DpnI (NEB) and purified using Invitrogen PCR purification kit. From the PCR reaction 5 µL of the template was mixed with 50 µL of chemically competent *E. coli* DH5α cells using heat shock transformation. After recovery in 200 µL of SOC medium, 100 µL of cells were plated onto LB plates with 50 µg/ml kanamycin and grown at 37 °C overnight. Five randomly selected colonies were grown in 5 mL of LB broth with 50 µg/ml kanamycin and grown over night in 37ºC shaking incubator at 250 RPM. Overnight culture was used to isolate the plasmid using Biobasic miniprep kit. Isolated plasmids were digested in a 50µL reaction consisting of 1 µg of plasmid template, 5 µL of cut-smart Buffer®, 20 U of BsaI-HF®, and topped up to 50 µL with nuclease-free water. Digest reaction was left to incubate at room temperature ~ 23 °C for 30 min and was then visualized on a 0.8% agarose gel. Plasmid with successful BsaI integration was used as a template for the integration of the second BsaI site.

The isolated plasmid was used as the template for the second round of PCR. In the second round of PCR, primers pFAB4876_frwd_2BsaI and pFAB4876_rev_2BsaI were used to introduce

the second BsaI site; 5'-GGTCTC-3' into the pFAB4876 backbone. PCR reaction was performed in 50 µl PCR using the same volumes and conditions as mentioned in the first round of PCR. The PCR reaction was purified using Invitrogen PCR purification kit then treated with DpnI (NEB) to remove methylated DNA template. 5µl of plasmid was transformed in 50µl of DH5α using heat shock transformation at 42°C for 30 seconds, and recovered with 200 µL of SOC media, and plated on pre-warmed 50 µg/ml kanamycin agar plate. Five randomly selected colonies were chosen and inoculated in 5 ml of LB broth with 50 µg/ml kanamycin and grown over night in 37°C shaking incubator at 250 RPM. Overnight culture was used to isolate the plasmid using Biobasic miniprep kit. Isolated plasmids were digested in a 50µL reaction consisting of 1µg of plasmid template, 5µL of cut-smart Buffer®, 20U of BsaI-HF®, and topped up to 50µL with nuclease-free water. Digest reaction was left to incubate at room temperature for 30 min and was then visualized on a 0.8% agarose gel. Plasmid with successful integration of second BsaI site was stored in 50% (v/v) glycerol solution for long term storage in -80°C freezer. The successful integration for two BsaI sites in pFAB4876 makes the plasmid golden gate compatible and was renamed pFAB.

Protocol S2: Preparation of cell lysate for cell-free protein synthesis reactions

To prepare the cell lysate for cell-free protein synthesis reactions (CFPS), we obtained the protocol from but made modifications to the protocol to fit our application.[87, 112] *E. coli* BL21Star™ (DE3) cells were acquired from a glycerol stock, streaked on an LB agar plate, and incubated overnight at 37 °C. A single colony of *E. coli* BL21Star™(DE3) was inoculated into a starter culture of 50 mL in LB with no selection, and grown overnight (15-18 h) at 37 °C and 200 rpm. A solution of 2x YTP was prepared by dissolving 5.0 g sodium chloride, 16.0 g of tryptone, 10.0 g of yeast extract, 7.0 g of potassium phosphate dibasic, and 3.0 g of potassium phosphate monobasic into

750 mL of ddH_2O. A glucose solution was prepared by dissolving 250 mL of ddH_2O with 18 g of D-glucose. 2xYTP was transferred to a 2 L baffled flask and autoclaved for 30 min at 121 °C. The glucose solution was filter sterilized using a 0.22 µm vacuum filtration system. On the day of inoculation, the glucose solution was added to the 2xYTP media and warmed in a 37 °C incubator. Overnight starter culture of BL21star™ (DE3) was removed from shaking incubator and diluted in a 1:10 ratio and OD_{600} was measured using a spectrophotometer. Overnight starter culture was added to 1L of 2xYTPG media and inoculated culture was incubated at 37 °C while shaking at 200 rpm. OD_{600} was monitored every hour to ensure stable growth until culture reached mid exponential phase or $OD_{600} = 0.6$. After reaching this OD, the culture was induced with 1 mL of 1 M isopropyl β-D-1-thiogalactopyranoside (IPTG) to a final concentration of 1 mM. After induction, the OD_{600} of the culture was monitored every 20-30 min and was immediately immersed in an ice-water bath to arrest growth at OD_{600} 1.9-2.0. The culture was transferred into cold 1 L centrifuge bottles (Beckman Coulter, Indianapolis, IN) and centrifuged for 10 min at 5000 x g and 4°C (Avanti® J-E Centrifuge, Beckman Coulter, Indianapolis, IN). Supernatant was removed, and the pellet was placed on ice using a sterile spatula and transferred to a cold 50 mL Falcon tube placed on ice. Cells were washed three times with 30 mL of cold S30 buffer (14 mM Mg $(OAc)_2$, 10 mM Tris (OAc), 60 mM KOAc, 2 mM dithiothreitol) by resuspension via vortexing with short bursts (20 - 30 s) with rest periods (1 min) in between. For each wash, the suspension was centrifuged at 5000 x g and 4°C for 10 minutes. After disposing the supernatant, the pellet was weighed, then flash frozen via liquid nitrogen and kept at – 80 °C until extract preparation. The frozen cell pellet was combined with 0.8 mL of S30 buffer per 1 gram of cell pellet and thawed on ice. Once the cell pellet was fully thawed, it was resuspended via vortexing, with short bursts (20 - 30 s) and rest periods (1 min), until no visible clumps were observed. 1 mL of resuspended cell

pellet was transferred to 1.5 ml Eppendorf tubes. A Q125 sonicator (Qsonica, Newtown, CT) with a 3.175 mm probe was used at a frequency of 20 kHz and resuspension was sonicated for 45 s followed by 59 s off for 3 total cycles, with amplitude set at 50 %. Immediately after, 4.5 µL of 1 M DTT was added to the lysate, Eppendorf tubes were closed and gently inverted 3-4 times. In total, 800-900 J of energy was delivered to each 1.5 mL microfuge tube containing 1mL of resuspended cells. Using a Pierce™ BCA assay kit (ThermoScientific), total protein concentration was measured of the lysate. To maintain consistency between batches, cell-extract was concentrated using a 10,000 MWCO centrifuge column (GE Healthcare; Vivaspin20) to obtain a final concentration of 15mg/ml. The lysate was then centrifuged using a tabletop centrifuge at 14,000 × g and 4 °C for 15 minutes. Following centrifugation, the supernatant (or lysate) was pipetted into new and sterile 1.5 mL Eppendorf tubes, flash frozen in liquid nitrogen, and kept in a – 80 °C freezer until use.

Protocol S3: Quantification of the Reporter Protein

Using a half area 96-well black polystyrene plate (Greiner, Germany), 48 µL of 0.05 M HEPES (pH 8) was loaded for each sample and replicates. Reactions are removed from 30°C incubator for endpoint measurement, and 2 µL were transferred into the 48 µL of 0.05 M HEPES, pH 8. Samples were pipetted up and down again in the well to mix. Once all reactions are loaded, the 96 well plate was placed in the ClARIOstar and the fluorescence was measured at an excitation wavelength of 488nm and an emission wavelength of 507nm using a fluorescence microplate reader (CLARIOstar, BMG Labtech, Germany). Using an eGFP standard curve, the concentration of eGFP can be calculated from the obtained fluorescence readings.

Protocol S4: Methods for Preparation of an eGFP Standard Curve

A standard curve of quantitation of eGFP was prepared in the following manner. From a glycerol stock of BL21(DE3) star™-eGFP was streaked on an agar plate with 100µg/ml carbenicillin selection and incubated at 37ºC overnight. A single colony was inoculated in 10ml of LB with 50 µg/ml carbenicillin in a round bottom test tube and grown over night at 37 °C and 250 rpm. 5ml culture was transferred to a 15ml falcon tube and centrifuged at 10,000 x g at 4ºC for 5 min. Supernatant was discarded, his-tag purification was carried out using HisPur™ cobalt resin (Invitrogen). Pellet was immersed in ice and 800 µl of wash buffer was added and was resuspended by pipetting up and down. Pellet was incubated on ice for 20-30 min, resuspension solution was transferred to 1.5ml microcentrifuge tubes and sonicated for 10s on, 10 s off, until the total J delivered was ~200 J. Sample was centrifuged at 10,000 x g for 5 min at 4ºC, supernatant was separated and collected in separate 1.5 mL microfuge tube. Cobalt purification columns were prepared by allowing the storage buffer to drip through and equilibrated the column with 2 column bed volumes of wash buffer (400 µL). 400µL of supernatant was transferred to spin column and bottom was plugged to prevent leakage and inverted six times. Spin column was placed on ice and ice box was placed on orbital shaker and incubated for 30 minutes. Bottom plug was removed, and spin column was centrifuged at 700 × g for 2 minutes at 4ºC to remove supernatant. Process was repeated again with the rest of 400µL of supernatant. The spin column was washed with two resin beds of wash buffer (400 µL) and centrifuged at 700 × g for 2 minutes at 4ºC and fractions were collected in a microcentrifuge tube. The spin column was washed three times, and each fraction was collected. Elution was performed by adding 2 resin beds of elution buffer (400 µL) and centrifuged at 700 × g for 2 minutes at 4ºC and fractions were collected in a microcentrifuge tube. Proteins were eluted from the spin column two more times and fractions were collected each time. The spin column was regenerated by washing with 10 resin bed volumes of MES buffer (20mM

2-(N-morpholine)-ethane sulfonic acid, 0.1M sodium chloride; pH 5.0) then centrifuging at 700 × g for 2 minutes at 4°C. Then washing the spin column with 10 resin bed volumes of ultrapure water and centrifuged at 700 × g for 2 minutes at 4°C. The cobalt resin was stored as 50% slurry and 20% ethanol and stored at 4°C. To remove imidazole from the purified protein dialysis was performed using Thermo Scientific™ Slide-A-Lyzer™ Dialysis Cassettes (Invitrogen) against dialysis buffer (150 m*M* NaCl, 100 m*M* HEPES–NaOH, pH 8.0) and concentrated using Amicon Ultra-15 concentrators (Millipore, Billerica, MA). Using Pierce BCA protein assay kit, the overall concentration of the purified protein was determined by measuring absorbance at 562nm, and extrapolating concentration from BCA standard curve. Serial dilutions of stock eGFP protein, ranging from 0 to 800µg/mL of protein was prepared in triplicates and was measured at 562nm to determine absorbance. Resulting measurements were used to plot a standard curve in order to convert fluorescence readings to concentration of eGFP in µg/mL as shown in **Figure S11**.

Table: *Escherichia coli* strains and plasmids used in this study

Strains/Plasmids	Description	Source/Reference
DH5α	F- ϕ80lacZΔM15 Δ(lacZYA-argF) U169 recA1 endA1 hsdR17 (rk- mk+) phoA supE44 λ- thi-1 gyrA96 relA1	Invitrogen
One Shot® BL21 Star™	F- ompT hsdSB(rB- mB-) gal dcm rne131 (DE3)	Invitrogen
JM109	endA1 glnV44 thi-1 relA1 gyrA96 recA1 mcrB+ Δ(lac-proAB) e14- [F' traD36 proAB+ lacIq lacZΔM15] hsdR17($r_K^-m_K^+$)	New England Biolabs
Plasmids		
pProm1_BCD1-GFP	Kan^R , p15A, sfGFP under constitutive promoter, 2-kb	Addgene (#80649)
pTU1	Amp^R , pBR322ori, 2-kb	Addgene (#72934)
pTU1_eGFP	Amp^R , pBR322ori,eGFP under constitutive T7 promoter, 3-kb	This study
pTU1_puuAp_egfp	Amp^R , pBR322ori,eGFP under PuuAp promoter, 3-kb	This study
pTU1_TacR(3)_egfp	Amp^R , pBR322ori,eGFP under TacR(3) promoter, 3-kb	
pTU1_TacR(2)_egfp	Amp^R , pBR322ori,eGFP under TacR(2) promoter, 3-kb	
pTU1_LR(2)_egfp	Amp^R , pBR322ori,eGFP under LR(2) promoter, 3-kb	
pTU1_P_{hyb}(1A)_egfp	Amp^R , pBR322ori,eGFP under P_{hyb}(1A) promoter, 3-kb	This study
pTU1_P_{hyb}(2A)_egfp	Amp^R , pBR322ori,eGFP under P_{hyb}(2A) promoter, 3-kb	This study
pTU1_P_{hyb}(3A)_egfp	Amp^R , pBR322ori,eGFP under P_{hyb}(3A) promoter, 3-kb	This study
pTU1_P_{hyb}(1B)_egfp	Amp^R , pBR322ori,eGFP under P_{hyb}(1B) promoter, 3-kb	This study
pTU1_P_{hyb}(2B)_egfp	Amp^R , pBR322ori,eGFP under P_{hyb}(2B) promoter, 3-kb	This study
pTU1_P_{hyb}(3B)_egfp	Amp^R , pBR322ori,eGFP under P_{hyb}(3B)) promoter, 3-kb	This study
pTU1_P_{hyb}(1C)_egfp	Amp^R , pBR322ori,eGFP under P_{hyb}(1C) promoter, 3-kb	This study
pTU1_P_{hyb}(2C)_egfp	Amp^R , pBR322ori,eGFP under P_{hyb}(2C) promoter, 3-kb	This study
pTU1_P_{hyb}(3C)_egfp	Amp^R , pBR322ori,eGFP under P_{hyb}(3C) promoter, 3-kb	This study
pFAB_PuuR	kan^R , p15Aori, PuuR under constitutive T7 promoter, 2.9-kb	This study

Table S2: DNA sequences used in this study

#	Name	Sequence	Source
1	T7_RBS	GGTCTCACTATCCCGCGAAATTAATACGACTCACTATAGGGGAATTGTGAGCGGATAACAATTCCCCTCTAGAAATAATTTTGTTTAACTTTAAGAAGGAGATATACCATAAGAGACC	72978[a]
2	Tag-linker	GGTCTCAGTACTTTAACTTTAAGAAGGAGATATATAAAAGAGACC	72982[a]
3	His-Tag	GGTCTCATAAATGCACCATCACCATCACCATAAGAGACC	72893[a]
4	BBa_B0015	GGTCTCATCGACCAGGCATCAAATAAAACGAAAGCGTTTATAGGCTCAGTCGAAAGACTGGGCCTTTCGTTTTATCTGTTGTTTGTCGGTGAACGCTCTCTACTAGAGTCACACTGGCTCACCTTCGGGTGGGCCTTTCTGCGTTTATATGTTAGAGACC	72998[a]
5	PuuR	GGTCTCACATATATGAGTGATGAGGGACTGGCGCCAGGAAAACGCTTGTCGGAAATCCGCCAGCAGCAGGGGCTTTCACAACGTCGTGCCGCCGAACTCTCCGGGCTGACTCACAGTGCTATCAGTACGATAGAACAAGATAAAGTCAGCCCTGCCATCAGTACGCTGCAAAAGCTGCTGAAGGTGTATGGTCTGTCACTCTCGGAATTCTTTTCCGAGCCGGAAAAACCTGATGAGCCGCAGGTCGTCATTAATCAGGACGACTTAATTGAGATGGGTAGTCAGGGTGTGTCAATGAAGCTGGTTCATAACGGTAACCCGAATCGCACGCTGGCGATGATCTTTGAAACGTACCAGCCGGGCACAACCACTGGGGAAAGAATTAAGCATCAGGGTGAGGAAATAGGCACTGTACTGGAAGGTGAAATTGTTCTGACGATTAATGGTCAGGATTACCACCTCGTCGCGGGGCAAAGTTATGCCATTAATACCGGCATCCCGCACAGTTTCAGTAATACGTCGGCAGGTATTTGCCGAATTATCAGCGCCCATACGCCCACCACGTTTTAAGGATCCTCGAAGAGACC	945886[b]
6	eGFP	GGTCTCACCGTCTCAATCTATCTGGAGTTGTCCCAATTCTTGTTGAATTAGATGGTGATGTTAATGGGCACAAATTTTCTGTCAGTGGAGAGGGTGAAGGTGATGCAACATACGGAAAACTTACCCTTAAATTTATTTGCACTACTGGAAAACTACCTGTTCCATGGCCAACACTTGTCACTACTTTCGGTTATGGTGTTCAATGCTTTGCGAGATACCCAGATCATATGAAACAGCATGACTTTTTCAAGAGTGCCATGCCCGAAGGTTATGTACAGGAAAGAACTATATTTTTCAAAGATGACGGGAACTACAAGACACGTGCTGAAGTCAAGTTTGAAGGTGATACCCTTGTTAATAGAATCGAGTTAAAAGGTATTGATTTTAAAGAAGATGGAAACATTCTTGGACACAAATTGGAATACAACTATAACTCACACAATGTATACATCATGGCAGACAAACAAAAGAATGGAATCAAAGTTAACTTCAAAATTAGACACAACATTGAAGATGGAAGCGTTCAACTAGCAGACCATTATCAACAAAATACTCCAATTGGCGATGGCCCTGTCCTTTTACCAGACAACCATTACCTGTCCACACAATCTGCCCTTTCGAAAGATCCCAACGAAAAGAGAGATCACATGGTCCTTCTTGAGTTTGTAACAGCTGCTGGGATTACACATGGCATGGATGAACTATACAAATAATCGAAGAGACC	72960[a]
7	PuuAp(WT)	GGTCTCACTATTCATTTTTGCAAACTCAATTTAACATTTGACAAACATTTAGTTTGCATACAGATTCGAATGGTGGTCATTATATTTTACGCTTTGGTACAGAGACC	This study
9	TacR(2)	GGTCTCACTATCTGTTGACAGTGGTCATTATATTTTACGCTATAATGTGTGGAGTGGTCATTATTTTACGCGTACAGAGACC	This study
16	TacR(3)	GGTCTCACTATCTGTTGACAATTAATCATCGGCTCGTATAATGTGTGGAGTGGTCATTATATTTTACGCGTACAGAGACC	This study
12	LR(2)	GGTCTCACTATATAAATTATCTCTGGCGGTGTTGACAGTGGTCATTATTATATTTTACGCGATACTGAGCACGTGGTCATTATATTTTACGCGTACAGAGACC	This study
17	P_{hyb}(3A)	GGTCTCACTATCTGTTGACAGTGGTCATTATATTTTACGCGATACTGAGCACAGTGGTCATTATATTTTACGCTTTGGAGCACGTGGTCATTATATTTTACGCGTACAGAGACC	This study
18	P_{hyb}(1B)	GGTCTCACTATCTGTTGACAATGTTCAATATTTTTTCAATGATACTGAGCACAGTGGTCATTATATTTTACGCTTTGGAGCACGTGGTCATTATATTTTACGCGTACAGAGACC	This study
20	P_{hyb}(2B)	GGTCTCACTATCTGTTGACAATGTTCAATATTTTTTCAATGATACTGAGCACAATGTTCAATATTTTTTCAATTTTGGAGCACGTGGTCATTATATTTTACGCGTACAGAGACC	This study
22	P_{hyb}(3B)	GGTCTCACTATCTGTTGACAATGTTCAATATTTTTTCAATGATACTGAGCACAATGTTCAATATTTTTTCAATTTTGGAGCACATGTTCAATATTTTTTCAATGTACAGAGACC	This study
19	P_{hyb}(3C)	GGTCTCACTATCTGTTGACAGTGGACTAAATTATCGCCATGATACTGAGCACAGTGGTCATTATATTTTACGCTTTGGAGCACGTGGTCATTATATTTTACGCGTACAGAGACC	This study
21	P_{hyb}(3C)	GGTCTCACTATCTGTTGACAATGTTCAATATTTTTTCAATGATACTGAGCACAATGTTCAATATTTTTTCAATTTTGGAGCACGTGGTCATTATATTTTACGCGTACAGAGACC	This study
23	P_{hyb}(3C)	GGTCTCACTATCTGTTGACAGTGGACTAAATTATCGCCATGATACTGAGCACAGTGGACTAAATTATCGCCATTTTGGAGCACGTGGACTAAATTATCGCCATGTACAGAGACC	This study

[a] Addgene gene number
[b] NCBI gene number
§Underlined regions are BsaI restriction sites

Table S3: List of PCR primers used in this study

(#)	Primer Name	Sequence 5'-3'
1	TacR(3)_1F	CACCAAGGTCTCACTATCTGTTGACAATTAATCATCGGCTC
2	TacR(3)_2F	CTGTTGACAATTAATCATCGGCTCGTATAATGTGTGGAGTGG
3	TacR(3)_1R	TGTGGAGTGGTCATTATATTTTACGCGTACAGAGACCTTGGTG
4	TacR(3)_2R	GCGTAAAATATAATGACCACTCCACACATTATACGAGC
5	P_{hyb}(1B)_2R	GCGTAAAATATAATGACCACGTGCTCCAAAGCGTAAAATATAATGACCACTGTGCTCA
6	P_{hyb}(1B)_R	CACCAAGGTCTCTGTACGCGTAAAATATAATGACCACGTGC
7	P_{hyb}(1B)_2F	CTGTTGACAATGTTCAATATTTTTTCATGATACTGAGCACAGTGGTCATTATATTTTACG
8	P_{hyb}(1B)_F	CACCAAGGTCTCACTATCTGTTGACAATGTTCAATATTTTTTCATGATAC
9	P_{hyb}(1C)_2R	CTGTTGACAGTGGACTAAATTATCGCCATGATACTGAGCACAGTGGTCATTATATTTTA
10	P_{hyb}(1C)_R	CTGTTGACAGTGGACTAAATTATCGCCATGATACTGAGCACAGTGGTCATTATATTTTA
11	P_{hyb}(1C)_2F	CTGTTGACAGTGGACTAAATTATCGCCATGATACTGAGCACAGTGGTCATTATATTTTA
12	P_{hyb}(1C)_F	CACCAAGGTCTCACTATCTGTTGACAGTGGACTAAATTATCGC
13	TacR(2)_2F	CTGTTGACAGTGGTCATTATATTTTACGCTATAATGTGTGGAGTGG
14	TacR(2)_1F	CACCAAGGTCTCACTATCTGTTGACAGTGGTCATTATATTTTACG
15	TacR(2)_2R	GCGTAAAATAATGACCACTCCACACATTATAGCGTAAAATATA
16	TacR(2)_1R	CACCAAGGTCTCTGTACGCGTAAAATAATGACCACTCCACA
17	P_{hyb}(2B)_2R	GCGTAAAATATAATGACCACGTGCTCCAAAATGAAAAAATATTGAACATTGTGCTCA
18	P_{hyb}(2B)_R	CACCAAGGTCTCTGTACGCGTAAAATATAATGACCACGTGC
19	P_{hyb}(2B)_2F	CTGTTGACAATGTTCAATATTTTTTCATGATACTGAGCACAATGTTCAATATTTTTTCATTTTG
20	P_{hyb}(2B)_F	CACCAAGGTCTCACTATCTGTTGACAATGTTCAATATTTTTTCATGATAC
21	P_{hyb}(2C)_2R	CTGTTGACAGTGGACTAAATTATCGCCATGATACTGAGCACAGTGGTCATTATATTTTA
22	P_{hyb}(2C)_R	CTGTTGACAGTGGACTAAATTATCGCCATGATACTGAGCACAGTGGTCATTATATTTTA
23	P_{hyb}(2C)_2F	CTGTTGACAGTGGACTAAATTATCGCCATGATACTGAGCACAGTGGTCATTATATTTTA
24	P_{hyb}(2C)_F	CTGTTGACAGTGGACTAAATTATCGCCATGATACTGAGCACAGTGGTCATTATATTTTA
25	P_{hyb}(3A)_2R	ATGAAAAAATATTGAACATGTGCTCCAAAATGAAAAAATATTGAACATTGTGCTCAGTAT
26	P_{hyb}(3A)_2R	GCGTAAAATATAATGACCACGTGCTCCAAAGCGTAAAATATAATGACCACTGTGCTCAGTATC
27	P_{hyb}(3A)_R	CACCAAGGTCTCTGTACGCGTAAAATATAATGACCACGTGC
28	P_{hyb}(3A)_F	CACCAAGGTCTCACTATCTGTTGACAGTGGTCATTATATTTTACGC
29	P_{hyb}(3B)_2F	GTTGACAGTGGTCATTATATTTTACGCGATACTGAGCACAGTGGTCATTATATTTT
30	P_{hyb}(3B)_R	CACCAAGGTCTCTGTACATGAAAAAATATTGAACATGTGCTCCAA
31	P_{hyb}(3B)_2F	TGTTGACAGTGGACTAAATTATCGCCATGATACTGAGCACAGTGGACTAAATTATCGCCATTTT
32	P_{hyb}(3B)_F	CACCAAGGTCTCACTATCTGTTGACAGTGGACTAAATTATCGC
33	P_{hyb}(3C)_2R	ATGGCGATAATTTAGTCCACGTGCTCCAAAATGGCGATAATTTAGTCCACTGT
34	P_{hyb}(3C)_R	CACCAAGGTCTCTGTACATGGCGATAATTTAGTCCACGTG
35	P_{hyb}(3C)_2F	TGTTGACAGTGGACTAAATTATCGCCATGATACTGAGCACAGTGGACTAAATTATCGCCATTTT
36	P_{hyb}(3C)_F	CACCAAGGTCTCACTATCTGTTGACAGTGGACTAAATTATCGC
37	PuuAp_1F	CACCAAGGTCTCACTATTCATTTTTGCAAACTCAATTTAACATTTGAC
38	PuuAp_2F	TCATTTTTGCAAACTCAATTTAACATTTGACAAACATTTAGTTTGCATACAGATTC
39	PuuAp_1R	CACCAAGGTCTCTGTACCAAAGCGTAAAATATAATGACCACCATT
40	PuuAp_2R	CAAAGCGTAAAATATAATGACCACCATTCGAATCTGTATGCAAACTAAATGTTTGTCAA
45	pFab4876_frwd_BsaI	AACGTCTCAATCTCTATAGAGACCCAATGTAGCACCTGAAGTCAGCC
46	pFab4876_rev_BsaI	GGGTCTCTATAGAGATTGAGACGTTTGAAGAGATAAATTGCACTGAAATCTAGAA
47	pFab4876_frwd_2BsaI	CGGTCTCATGTTTTAGAGAGACGTTACTAGTGCTTGGATTCTCACC
48	pFab4876_rev_2BsaI	CGTCTCTCTAAAACATGAGACCGACAACTTATATCGTATGGGGCT
49	PuuR_F	CACCAAGGTCTCACATATGATGAGTGATGAGGGACTGGC
50	PuuR_R	CACCAAGGTCTCTTCGAGGATCCTTAAAACGTGGTGGGCGTATG
51	pFAB_delphos_FRWD	GGATCGGTTGTCGAGTAAGGATC
52	pFAB_delphos_REV	TCATGCACAGGAGACTTTCTAATG
53	L440	AGCGAGTCAGTGAGCGAG
54	pBp_ECOR1	AAAAATAGGCGTATCACGAGGC

Table S4: Volumes and thermocycle conditions for PCR

Colony PCR

Phusion Master Mix	16.8 µL
Forward Primer	1.0 µL
Reverse Primer	1.0 µL
Template (colony dissolved in 20µL H_2O)	1 µL
Phusion	0.2 µL
Total	20.0 µL

Template Conditions

Phusion Master Mix	43.5 µL
Forward Primer	2.5 µL
Reverse Primer	2.5 µL
Template (colony dissolved in 20µL H_2O)	1.0 µL
Phusion	0.5 µL
Total	50.0 µL

Thermocycler Conditions

Step	Number of Cycles	Temperature	Time
Initial Denaturation	1	98 °C	30 s
Denaturation	35	98 °C	10 s
Annealing		45 °C -72 °C	20 s
Extension		72 °C	30 s
Final Extension	1	72 °C	10-12 min
hold	1	4 °C-10 °C	∞

Table S5: Golden Gate Conditions

Temperature	Time	Number of cycles
37 °C	5 min	15-30
16 °C	10 min	
50 °C	5 min	1
80 °C	5 min	1

Table S6: PuuR binding regions for our synthetic promoters

Binding Region	Sequence	Source
A	GTGGTCATTATATTTTACGC	*96, 97, 125*
B	ATGTTCAATATTTTTTCAAT	*96, 97, 125*
C	GTGGACTAAATTATCGCCAT	*126*

Table S7. Costs of reagents and materials for producing in-house cell-free extract

Chemical	Mass	Price
$Mg(OAc)_2$	50g	22.30
K(OAc)	1kg	223.00
Tris (OAc)	500g	149.0
IPTG	5g	66.00
DTT	5g	24.00
tRNA	100mg	219.00
Folinic Acid	100mg	142.00
NTPs	4x200µL	297.00
Oxalic Acid	5g	38.90
NAD	1g	124.00
PEP	25mg	227.00
Acetal CoA	25mg	129.00
K(Glu)	500g	249.00
$Mg(Glu)_2$	250g	83.00
NH4(Glu)	100g	255.28
Spermidine	5g	197.00
HEPES	25g	55.00
Cell-Free 20 aa mix	1mlx100mM of each amino acid	372.00
LB-Media	1L*4	43.00
Total		3044.20
Price per Reaction		1.52

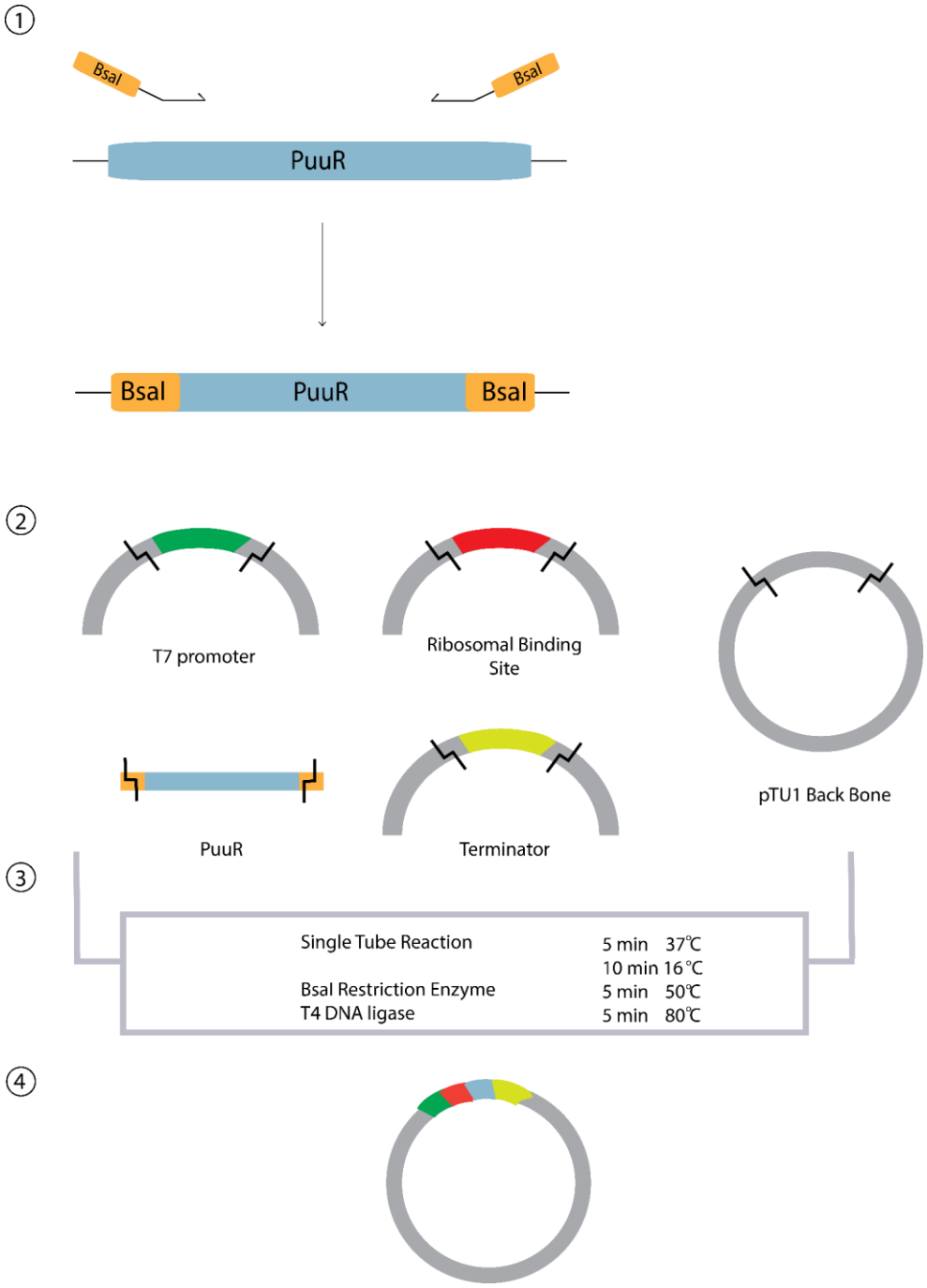

Figure S1- Repressor plasmid construction. Step (1): Flanking primers with BsaI restriction sites are used to amplify the PuuR insert. (2) Genetic parts are isolated: T7 promoter (green), RBS (red), PuuR insert (blue with orange flanking sites), terminator (yellow), and pTU1 backbone. All parts have two BsaI cut sites (shown as the 'Z'-block black line). (3) All genetic components are mixed in a single tube reaction with a BsaI restriction enzyme, T4 DNA ligase and subjected to thermocycler reactions conditions. (4) Final product of Golden Gate assembly reaction plasmid with all the integrated genetic components.

A

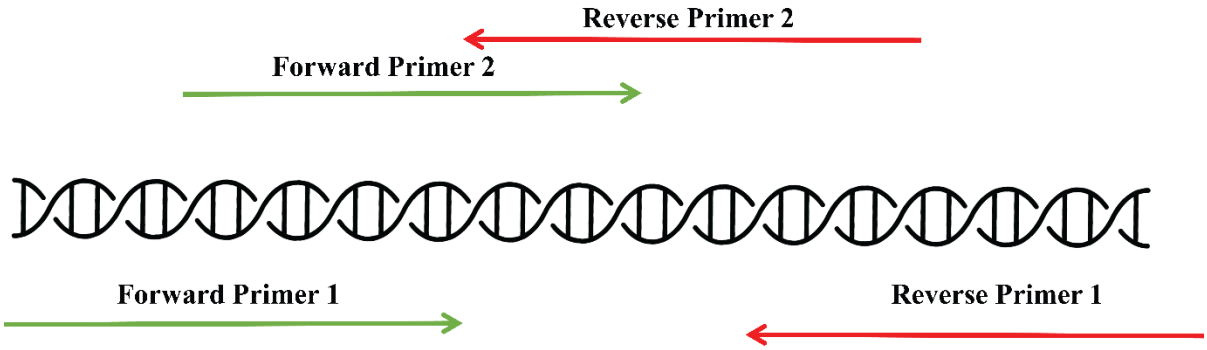

B

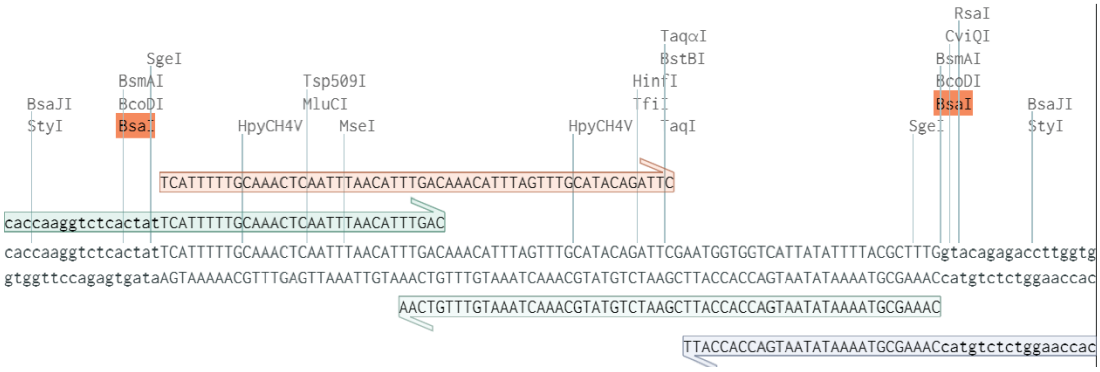

Figure S2 - Construction of promoter library. (A) Schematic of the required primers to construct the putrescine synthetic promoter library. Forward primer 2 and Reverse primer 2 are used to amplify the core promoter. The forward primer 1 and reverse primer 1 are used to flank the promoter with BsaI restriction sites. (B) A snippet of the DNA sequence for PuuAp promoter with the forward primer 1 (green) and 2 (orange) and reverse primer 1 (blue) and 2 (light green).

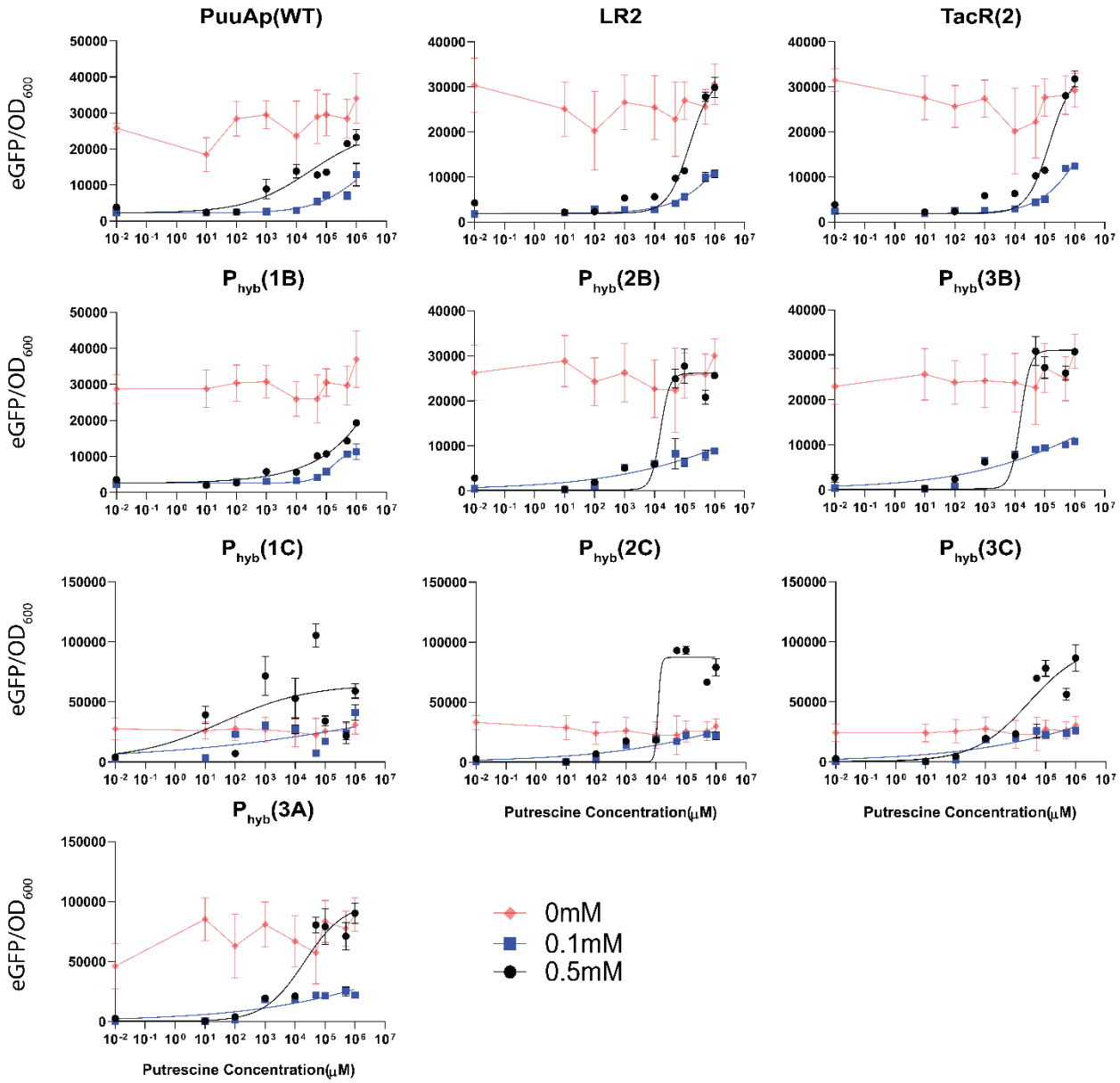

Figure S3 – Repression dynamics. Repressor expression was induced with IPTG at two concentrations 0.1 and 0.5 mM. The putrescine was exogenously added at a final concentration of (0, 0.01, 0.1, 1, 10, 100, 1000, 10000mM). Each point represents eGFP fluorescent output measured at the end of a 16 h incubation period and normalized to their OD. Semi-log curves were fitted by Prism 9.0 using a 4-parameter non-linear regression function. Fluorescent measurements were done in triplicates and error bars are representing one standard deviation.

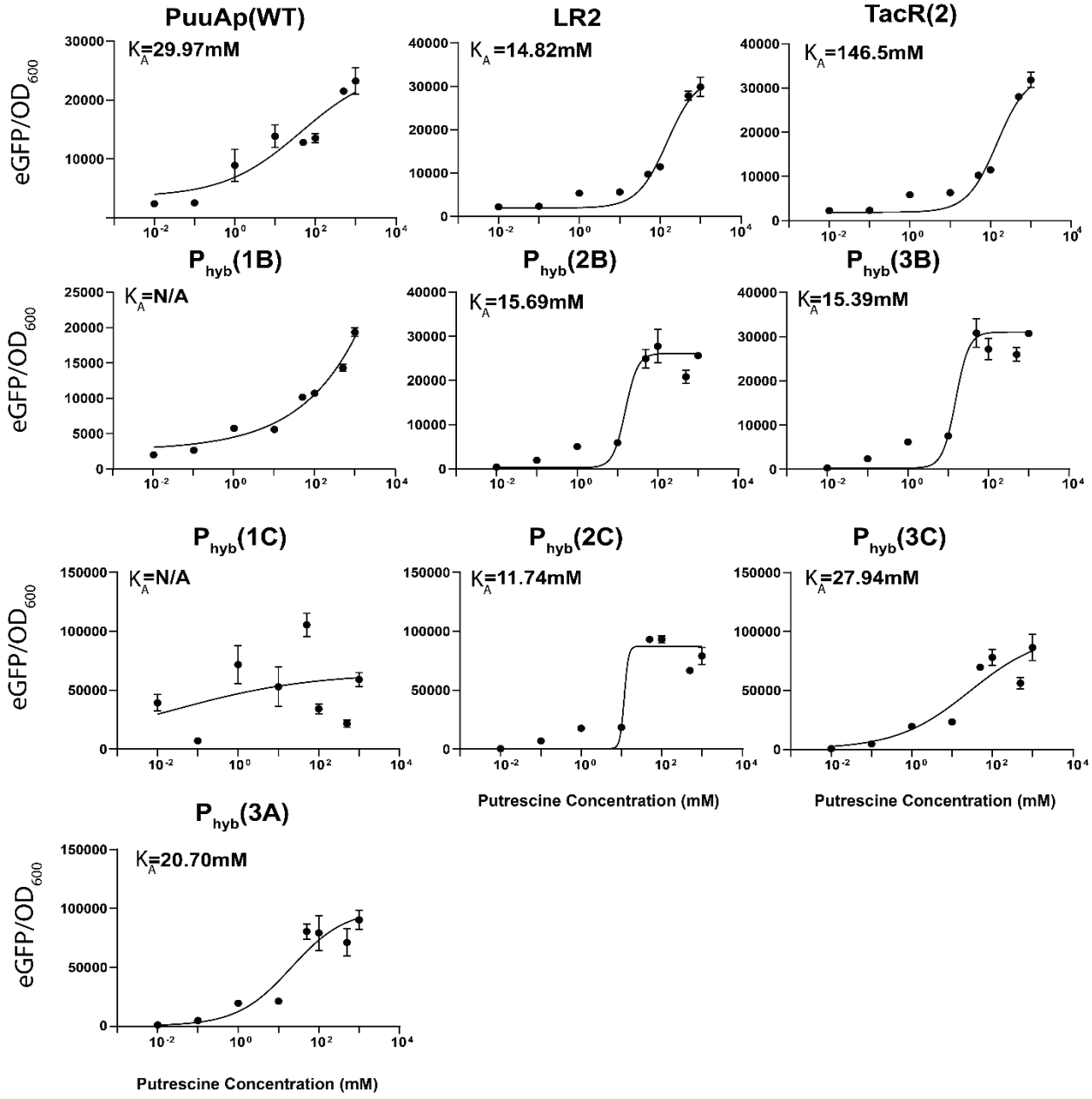

Figure S4 - Dose-response curves for our synthetic promoters. Each promoter was induced with 0.5 mM IPTG and with putrescine at a final concentration of 0, 0.01, 0.1, 1, 10, 100, 1000, 10000 mM. Each point represents an eGFP fluorescent output measured at the end of a 16 h incubation period and normalized to their OD. Semi-log curves were fitted by Prism 9.0 using a 4-parameter non-linear regression to determine the K_A. Fluorescent measurements were done in triplicates and error bars are representing one standard deviation.

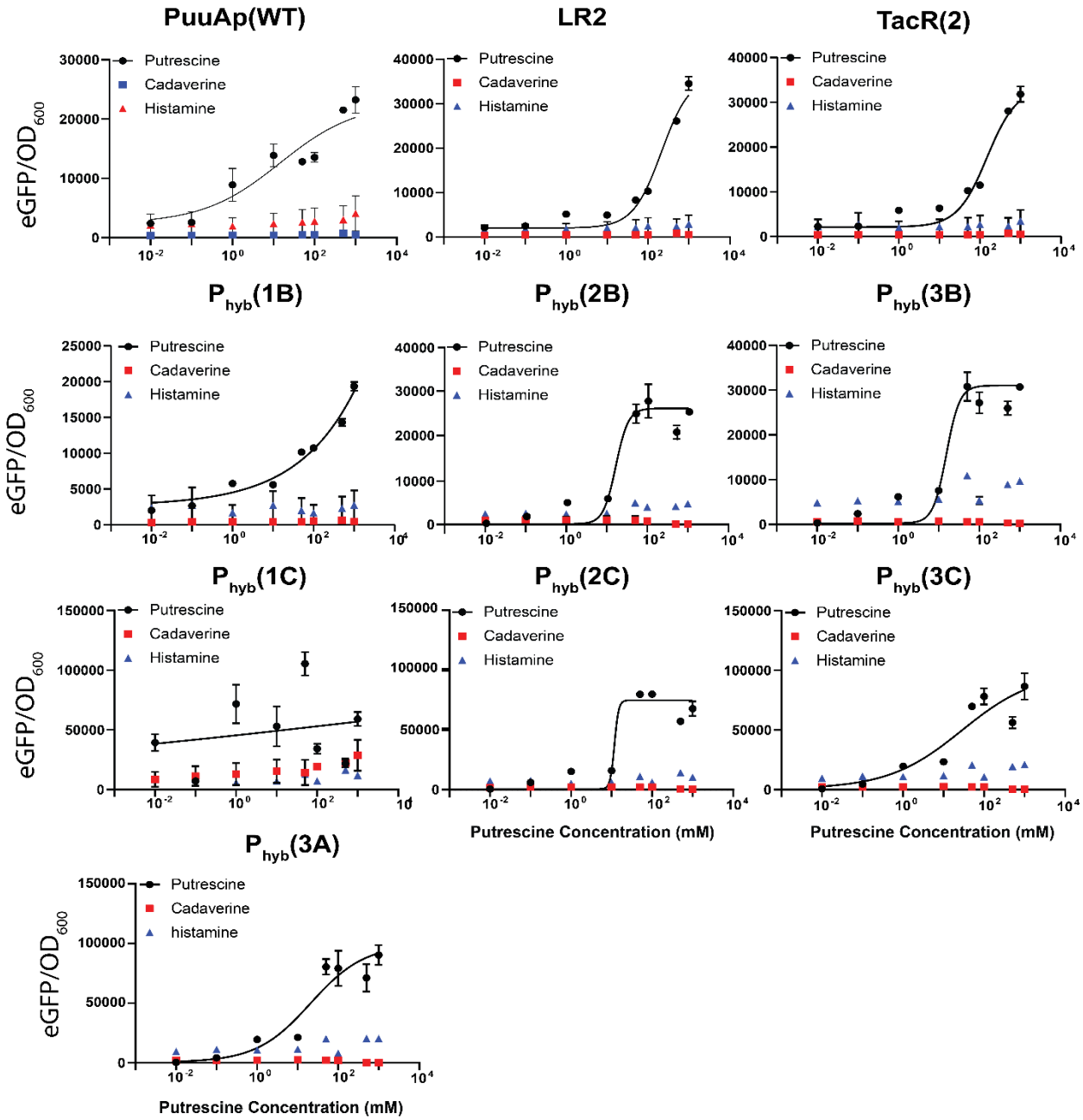

Figure S5 – Specificity testing for our synthetic promoters. Each promoter was induced with 0.5 mM IPTG and different concentrations of putrescine (black) and other chemically similar biogenic amines cadaverine (red) and histamine (blue) at a final concentration of 0, 0.01, 0.1, 1, 10, 100, 1000, 10000 mM. Each point represents eGFP fluorescent output measured at the end of a 16 h incubation period and normalized to their OD. Semi-log curves were fitted by Prism 9.0 using a 4-parameter non-linear regression to determine the K_A. Fluorescent measurements were done in triplicates and error bars are representing one standard deviation.

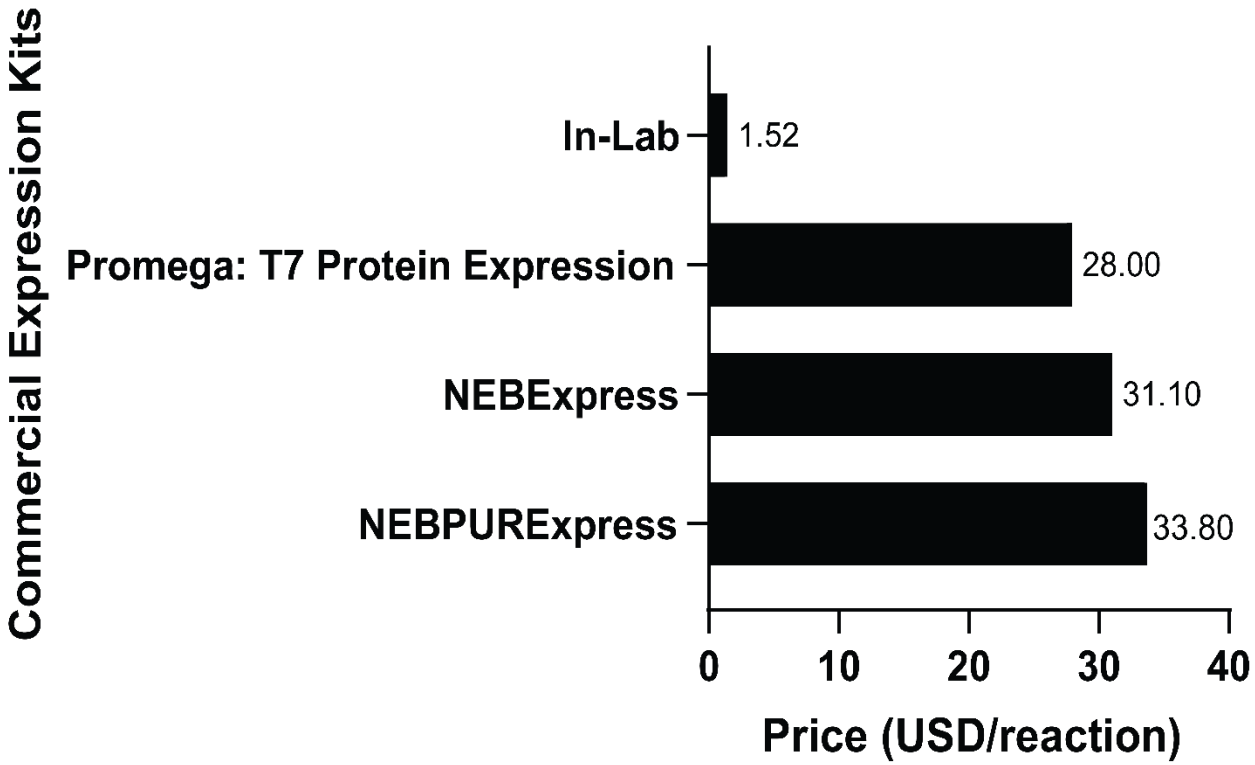

Figure S6 - Cost comparison of our cell-free extract with other commercial kits. The bar graph shows the price per reaction for each cell-free crude kit.

A

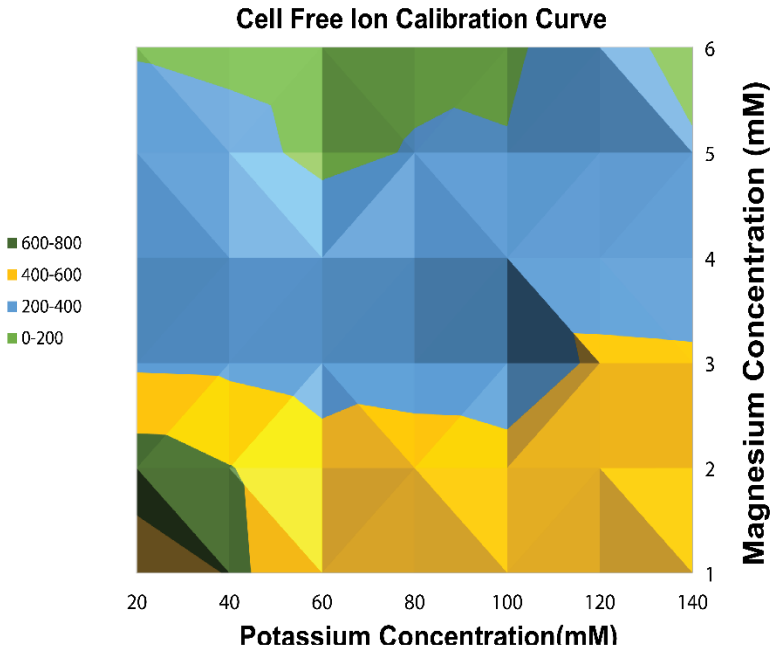

B

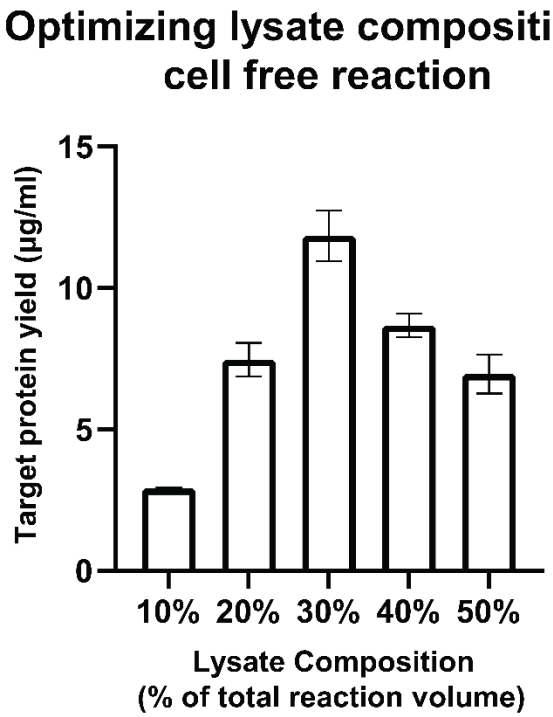

Figure S7 – Optimization of our in-house cell-free system. A) K^+ and Mg^{+2} ions were screened against a lysate with a eGFP protein concentration of 15 µg/mL as the optimal concentration for the expression of eGFP. All cell free reactions were performed in triplicates in 15 µL volumes. Endpoint fluorescence of each reaction was used to generate contour plot. eGFP fluorescence shows maximum at 2 mM of Mg^{+2} and 20 mM of K^+. B) Optimization of eGFP

protein yield by changing lysate composition. Error bars show one standard deviation for three independent biological replicates.

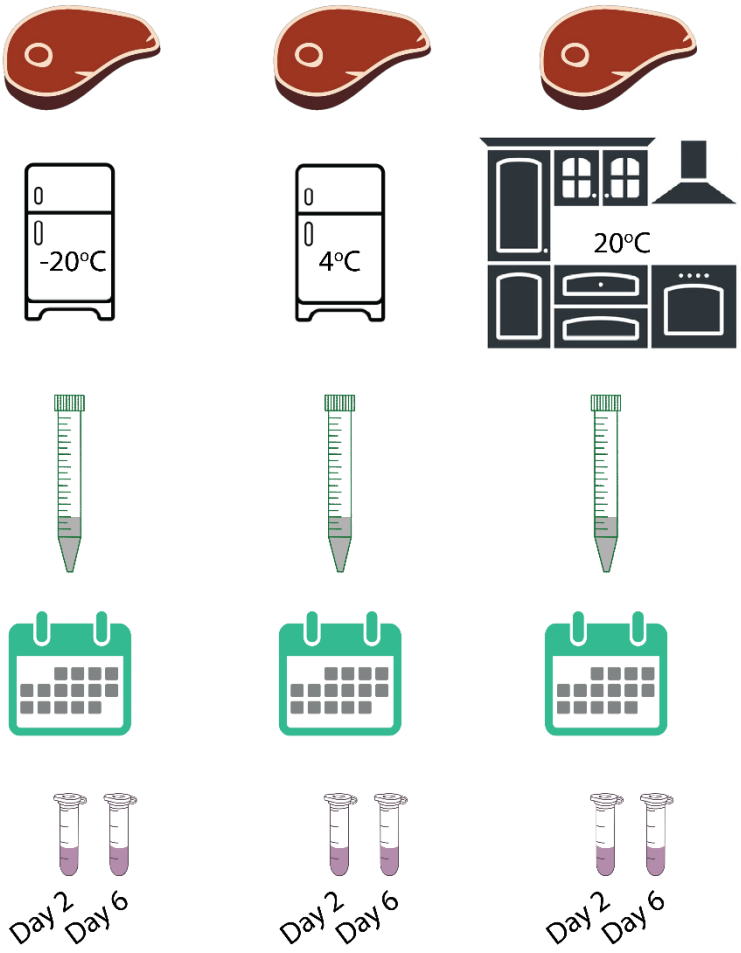

Figure S8 – Workflow showing meat sample preparation. 5 g of sample was collected from chicken breast, salmon fillet, and beef steak. Samples were transferred to a falcon tube and subjected to different storage temperature: 4 ˚C, 22 ˚C, and -20 ˚C. Samples were collected on the second day and sixth day for putrescine detection using our cell-free biosensor.

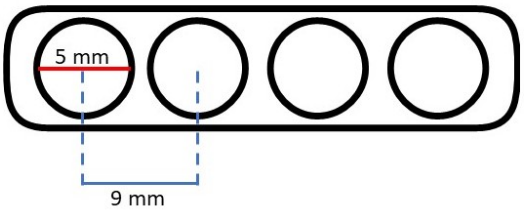

Figure S9 – FRSH paper disc device for assessing meat spoilage. Four 5 mm discs were fabricated 9 mm apart to match the well-to-well dimensions on the well-plate.

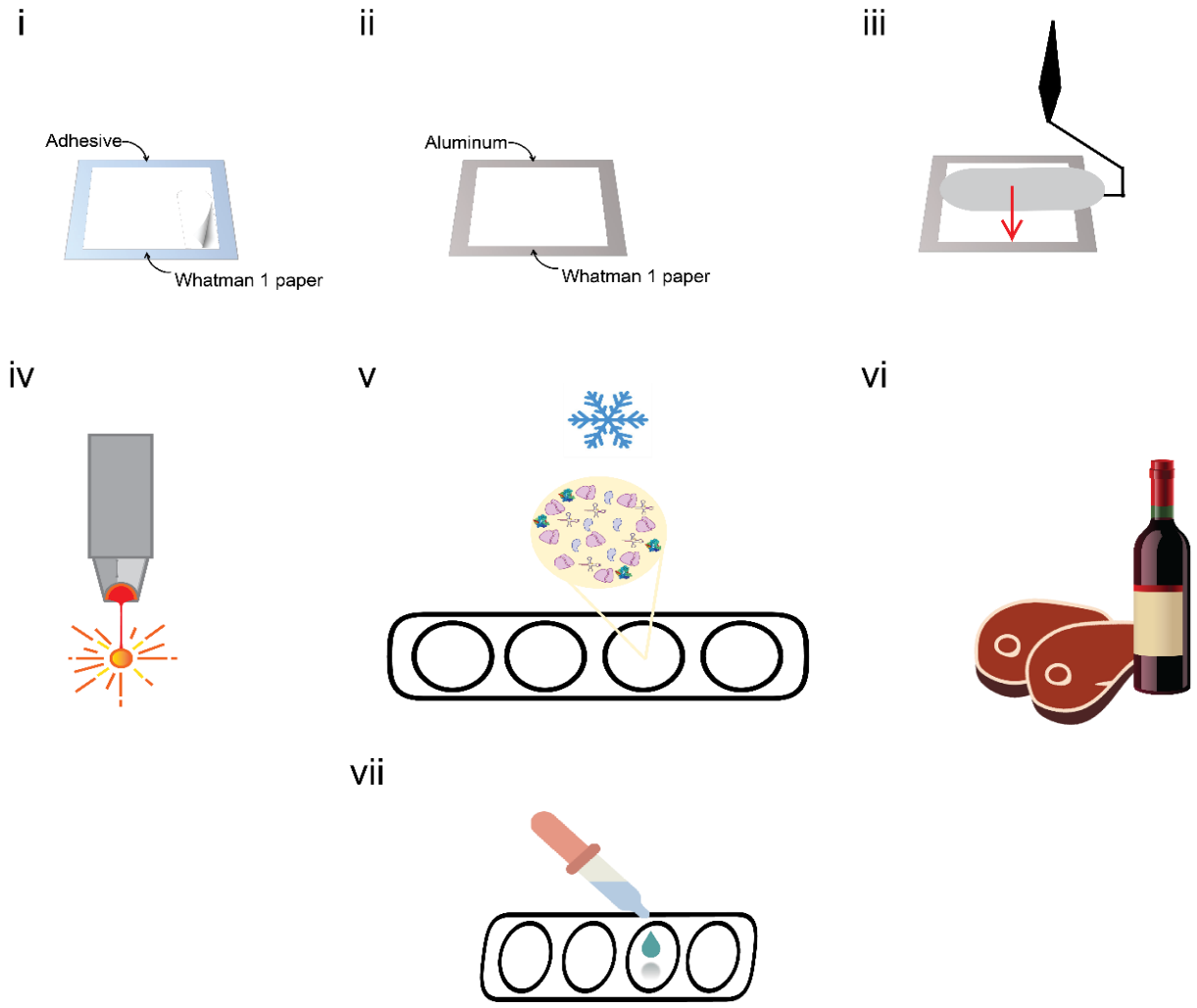

Figure S10 – FRSH device fabrication and sample testing. Step (i): An adhesive (20cmx20cm) is transferred to *Whatman Grade 1 Chr* paper and then gently peeled off. (ii) Whatman paper is transferred onto aluminum sheet (20cmx20cm). (iii) The foil-backed paper was fed through a manual cold-roll laminator. (iv) The paper aluminum substrate is used for laser cutting paper microfluidic device. (v) Cell free reactions are lyophilized on the paper discs. (vi) Samples are prepared for spoilage assessment. (vii) Food samples are loaded onto the discs to rehydrate and initiate the cell free reactions to yield an eGFP output.

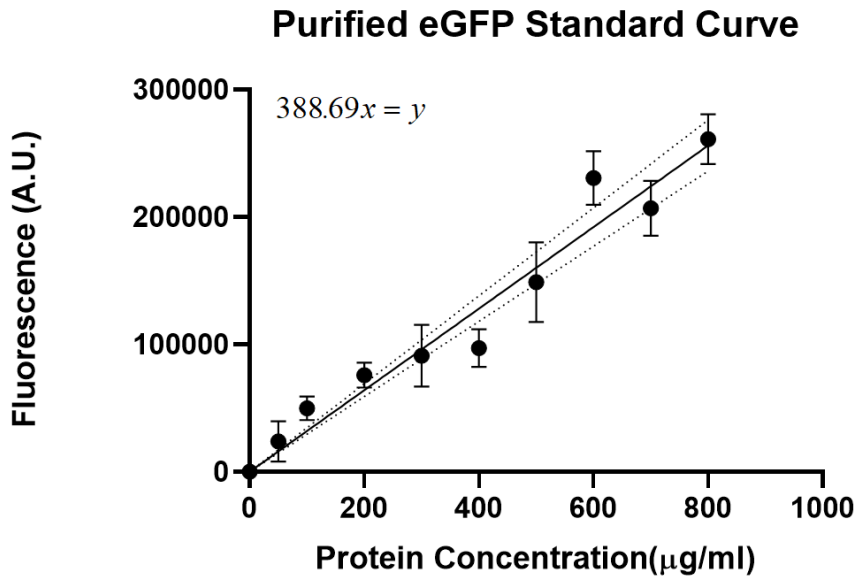

Figure S11 – eGFP calibration curve. eGFP protein was expressed and purified according to Supplementary Protocol S4. This calibration curve was used to convert fluorescence into eGFP yield (μg/mL). The error bars represent one standard deviation for three biological replicates.